

Nonlinear Distortion Suppression in Fiber
Optic Links Using Injection-Locked
Semiconductor Lasers

Nonlinear Distortion Suppression in Fiber
Optic Links Using Injection-Locked
Semiconductor Lasers

2000 12



Nonlinear Distortion Suppression in Fiber Optic Links Using Injection-Locked Semiconductor Lasers

By

Sung, Hyuk-Kee

Submitted in Partial Fulfilment of the
Requirements for the Degree
Master of Science

Department of Electrical and Electronic Engineering
The Graduate School

Yonsei University
Seoul, Korea
2000

감사의 글

지내고보니 길지않은 2년여의 대학원 생활의 결실인 이 논문을 작성하기까지 몰심양면으로 많은 도움과 격려를 아끼지 않으신 주위의 여러분들께 진심으로 감사드립니다. 가장 먼저 부족한 저를 잘 이끌어주시고 지도해주신 지도교수님이신 최우영 교수님께 감사를 드립니다. 그리고 저의 논문을 심사해주시고 세심하게 다듬어주신 한상국 교수님과 KIST의 전영민 박사님께 감사드립니다. 또한 학부때부터 대학원에 이르는 6년의 기간동안 저에게 많은 가르침을 주신 김봉열 교수님, 박규태 교수님, 차일환 교수님, 이상배 교수님, 강창언 교수님, 이문기 교수님, 박민용 교수님, 윤대희 교수님, 김재희 교수님, 이용석 교수님, 이재용 교수님, 김재석 교수님, 홍대식 교수님, 송홍엽 교수님, 이철희 교수님, 강문기 교수님, 이충용 교수님, 한건희 교수님께도 감사드립니다.

연구실의 최고참이신 정태형, 먼저 졸업하셨지만 항상 영원한 연구실의 맏형으로 남아있는 ETRI에 계신 태식이형, 저와 같이 졸업하는 다재다능하신 선배님 경환이형, 꼼꼼하고 항상 무언가 노력하는 모습을 보여주시는 승우형, 연구에 있어서라면 누구에게도 뒤지지않는 그리고 이 논문에도 많은 도움을 주신 영광이형, 동기로서 대학원생활에 많은 도움을 준 조용하지만 예리한 재욱이, 연구실의 살림꾼이자 활력소인 유근이, 창조적인 아이디어의 소유자 용상이, 연구에도 다른 일에도 항상 열심인 창순이, 굳은 일을 도맡아하는 준혁이, 연구실의 멋장이 기억이, 먼저 졸업하신 민우형, 용호형, 세은이형, 성훈이, 명수에게도 감사의 말을 전합니다.

그리고 대학생활의 낭만을 함께 했던 친구들, 영건이, 태곤이, 재범이, 기대, 상업이, 영철이, 윤서, 춘이에게도 아울러 감사의 마음을 전합니다.

마지막으로 항상 멀리 떨어져있는 저를 걱정해주시고 염려해주신 저의 마음의 안식처인 부모님과 저에게 늘 큰 힘이 되어준 누님께 진심으로 감사의 마음을 전합니다.

이천년 십이월

성혁기



Index

Figure Index	-----	ii
Table Index	-----	iv
Abstract	-----	v
I. Introduction	-----	1
II. Nonlinear Distortion Characteristics of Injection-locked DFB-LD	- 3	
A. Locking Characteristic Analysis	-----	3
B. Nonlinear Distortion Suppression in Injection-locked DFB-LD	-	11
III. IMD3 Reduction of Injection-locked FP-LD	-----	19
A. Injection-locking Bandwidth of FP-LD	-----	19
B. Dynamic Range Enhancement	-----	26
VI. Fiber Dispersion-induced IMD3 over Fiber Transmission	-----	31
A. IMD3 for DFB-LD	-----	31
A-1. Experiments	-----	31
A-2. Simulations	-----	40
B. IMD3 for FP-LD	-----	41
V. Conclusion	-----	51
IV. References	-----	54
Abstract (in Korean)	-----	57

Figure Index

Fig. 2-1. Characteristics of locking regimes	7
Fig. 2-2. Power spectra for the different locking conditions	9
Fig. 2-3. Frequency responses both the free-running and injection-locked lasers	15
Fig. 2-4. Simulated RF Power spectra of the DFB-LD	16
Fig. 2-5. The SFDR of the link with directly modulated DFB-LD for the free- running and injection-locked laser	18
Fig. 3-1. Experimental setup	20
Fig. 3-2. Optical power spectra of FP-LD and definition of mode number –	22
Fig. 3-3. Injection locking bandwidth versus mode number	24
Fig. 3-4. Frequency detuning versus the ML output power	25
Fig. 3-5. Measured RF power spectra	27
Fig. 3-6. Measured FP-LD output RF component and IMD3 versus modulating input RF power	29
Fig. 3-7. Normalized SFDR improvement for all injection target modes -	30
Fig. 4-1. Experimental setup	32
Fig. 4-2. Measured RF power spectra for the free-running DFB-LD --	34
Fig. 4-3. Measured RF power spectra for the injection-locked DFB-LD -	35
Fig. 4-4. Optical spectra measured by Fabry-Perot interferometer for the free- running and injection-locked DFB-LD	37
Fig. 4-5. Received RF power and IMD3 for the free-running DFB-LD -	38
Fig. 4-6. Received RF power and IMD3 for the injection-locked DFB-LD -	39
Fig. 4-7. Numerical Simulation of fiber distortion-induced IMD3	42

Fig. 4-8. Measured RF power spectra for the free-running FP-LD	-----	43
Fig. 4-9. Measured RF power spectra for the injection-locked FP-LD	---	44
Fig. 4-10. Optical spectra measured by Fabry-Perot interferometer for the free- running and injection-locked FP-LD	-----	46
Fig. 4-11. Received RF power and IMD3 for the free-running FP-LD	-	47
Fig. 4-12. Received RF power and IMD3 for the injection-locked FP-LD	-	50
Fig. 4-13. Fiber dispersion-induced IMD3 reduction by optical injection locking	-----	52

Table Index

Table I. Laser Parameter and Their Numerical Values	-----	6
Table II. Laser Parameter Value for IMD3 Analysis	-----	13

Abstract

Nonlinear Distortion Suppression in Fiber Optic Links Using Injection-locked Semiconductor Lasers

Sung, Hyuk-Kee

Dept. of Electrical and Electronic Eng.

The Graduate School

Yonsei University

In SCM fiber optic systems using direct modulation of the lasers, semiconductor laser nonlinearities and fiber chromatic dispersion cause harmonic and intermodulation distortions, and these can severely degrade overall system performance. As one method for suppressing the semiconductor laser nonlinearities and, thus, IMD3, optical injection locking of semiconductor lasers is very effective.

In this paper, through the small-signal analysis of the rate equation, injection locking characteristics are theoretically analyzed, and the effects of optical injection locking on the injection locking bandwidth and IMD3 suppression in a side-mode injection-locked FP-LD are experimentally investigated. It is shown that FP-LD injection locking bandwidth and reduction of IMD3 is varied at the different injection target mode of FP-LD. Injection locking bandwidth and reduction of IMD3 can be enhanced by choosing an appropriate injection target mode.

The dispersion-induced IMD3 variations in fiber optic link IMD3 on fiber transmission length are experimentally investigated for the free-running and injection-locked DFB- / FP-LD. IMDs in fiber optic link are degraded over transmission through dispersive fiber due to the combined effect of the laser nonlinearities and fiber dispersion. On the contrary, because the injection-locked semiconductor lasers have the improved laser dynamics such as the relaxation oscillation frequency increase and the reduced frequency chirping, the significant IMD3 reduction can be achieved, and the dispersion-induced IMD3 of the injection-locked DFB- / FP-LD is maintained not being degraded over fiber transmission.

Key words : laser nonlinearity, fiber chromatic dispersion, intermodulation distortion, optical injection locking

I. Introduction

At information technology age, it is optical communication technology that provides large data capacity and high-speed transmission which information consumers need. Optical transmission techniques up to several tens of Gbps have been already applicable and are used in the field of multimedia data transmission. Furthermore, the rapidly growing popularity of the Internet and the World Wide Web requires more rapid and capacity-enhanced optical communication networks.

Among many optical communication systems, subcarrier multiplexed (SCM) fiber optic systems with direct laser intensity modulation have many applications such as wireless local loop, cable television distributions and fiber-radio systems. The direct modulation of semiconductor laser is a simple, low-cost approach for transmitting RF-range subcarriers. However, in the system where directly modulated semiconductor lasers are used, the nonlinear distortions such as harmonic distortions and intermodulation distortions due to semiconductor laser nonlinearities and fiber chromatic dispersion can severely degrade overall system performance [1-3]. Among many distortions, in the systems where 2HD and IMD2 frequencies all lie outside the frequency band of interest, the overall system performance is mainly affected by IMD3 [4], although third-order intermodulation distortion (IMD3) is much smaller than second-order harmonic (2HD) and sum term intermodulation distortion (IMD2) [5].

Hence, it is required to suppress the IMD3 induced by semiconductor laser nonlinearities and fiber dispersion. Several techniques have been proposed to

reduce the dispersion-induced distortions in SCM fiber optic systems such as using fiber grating equalizers [6] or tilted etalon [7]. Also as another solution for suppressing nonlinearities of semiconductor lasers, the optical injection locking of semiconductor lasers has been widely investigated and found very effective [8-9]. The optical injection locking scheme requires two light sources - master laser (ML) and slave laser (SL). The light from ML is injected into SL and SL's output is locked to ML. Two major parameters for the injection locking are frequency detuning - frequency difference between ML and SL - and injection power ratio. If the injection locking conditions are satisfied, improvements in laser dynamics such as relaxation oscillation frequency increase and frequency chirp reduction can be achieved [10]-[11].

However, the effect of fiber dispersion-induced IMD3 under optical injection locking has not been studied in the fiber optic link. In this thesis, the fiber dispersion-induced IMD3s under free-running and injection-locked state are investigated. First, Section II deals with nonlinear distortion characteristics of injection-locked distributed feedback laser diode (DFB-LD) based on numerical analysis. In section III, injection locking bandwidth and IMD3 reduction of injection-locked Fabry-Perot laser diode (FP-LD) with no fiber transmission is investigated experimentally. Finally, Section IV deals with the experimental investigation on the dispersion-induced IMD3 using free-running DFB- / FP-LD and demonstrate that the dispersion-induced IMD3 can also be much reduced and made less dependent on the transmission length by using injection-locked DFB- / FP-LD.

II. Nonlinear Distortion Characteristics of Injection-locked DFB-LD

A. Locking Characteristic Analysis

Injection locking is a way to synchronize one free-running oscillator to a stabilized master oscillator. Injection locking of semiconductor lasers can be widely used in many optical communication systems because it is a good method to improve semiconductor laser characteristics such as frequency chirping reduction, partition noise reduction, linewidth narrowing and relaxation oscillation frequency increase [9,12]. Optical injection locking method requires two optical sources, - a master laser (ML) and a slave laser (SL). Light emitted from one laser, the ML, is injected into the other laser, the SL, and the reflected light from the SL is assumed to be blocked by optical isolator or circulator. The light from the ML is injected into the SL and the SL's output is locked to the ML when the injection locking conditions are met. Two major parameters for the injection locking are frequency detuning - frequency difference between the ML and the SL - and injection power ratio. If the injection locking conditions are satisfied, improvements in laser dynamics such as relaxation oscillation frequency increase and frequency chirp reduction can be achieved.

The optical injection locking is described by the following differential equation for the complex electric field of the SL [10,13] ;

$$\frac{d}{dt} E_{SL}(t) - \left\{ j\omega(N) + \frac{1}{2} \left[G(N) - \frac{1}{\tau_p} \right] \right\} E_{SL}(t) = \mathbf{h} f_a E_{ML}(t). \quad (1)$$

This equation is derived from a traveling wave description of the field inside the laser cavity. In the above equation, $E_{SL}(t)$ and $E_{ML}(t)$ represent the SL and ML electric field, respectively. $\omega(N)$ is the angular optical frequency and $G(N)$

the modal gain of the SL, both depending on the carrier density N . t_p is the photon lifetime, f_d the longitudinal mode spacing, and \mathbf{h} the coupling efficiency. The complex field of each laser is given by following equations;

$$E_{SL}(t) = E_0(t) e^{j[\omega_0 t + \mathbf{f}_0(t)]} \quad (2a)$$

$$\mathbf{h} E_{SL}(t) = E_1 e^{j[\omega_1 t + \mathbf{f}_1]} \quad , \quad (2b)$$

where $E_0(t)$, E_1 , $\mathbf{f}_0(t)$ and \mathbf{f}_1 are real-valued and ω_0 is the angular frequency of the free-running SL. E_1 and \mathbf{f}_1 is set to constant and zero respectively without loss of generality [10]. Phase noise can be neglected because the ML is intended to be a stabilized light source with narrow linewidth.

By means of the above equations and relationships between carrier density change and angular optical frequency of the SL, Eq.(1) can be converted to the amplitude-phase representation;

$$\frac{d}{dt} E_0(t) = \frac{1}{2} G_N \Delta N(t) E_0(t) + f_d E_1 \cos(\Delta(t)) \quad (3a)$$

$$\frac{d}{dt} \mathbf{f}_0(t) = \frac{1}{2} \mathbf{a} G_N \Delta N(t) + f_d \frac{E_1}{E_0(t)} \sin(\Delta(t)) \quad (3b)$$

$$\frac{d}{dt} N(t) = J - \frac{N(t)}{t_s} - G(N) E_0^2(t). \quad (3c)$$

In the above equations, G_N is gain coefficient, \mathbf{a} linewidth enhancement factor, $\Delta N(t)$ the relative change in carrier density, J injection term, and t_s the spontaneous emission lifetime. Equations (3a)-(3c) form the basic theoretical model for injection locking. Stationary solution from the above rate equation, injection locking bandwidth $\Delta \omega_L$ can be derived as follows where \tilde{E}_0 is stationary value of $E(t)$ [13],

$$|\Delta \omega_L| \leq f_d \frac{E_1}{\tilde{E}_0} \sqrt{1 + \mathbf{a}^2} \quad . \quad (4)$$

Injection locking bandwidth can be further classified into two distinctive

regimes: stable locking and unstable locking. In the stable locking regime, the output power converges to a steady-state value when a small perturbation is introduced. In the unstable locking regime, however, the power does not converge to the steady-state value but experiences a self-sustained oscillation or even chaos when a small perturbation is introduced [14]. Such an oscillation and chaos produce multiple sidebands in the output optical spectra. The range for the stable locking regime can be determined by the s-domain stability analysis of the rate equation.

Fig. 2-1 shows the stable locking range (S) for the frequency detuning between the ML and SL as a function of injection power ratio. The parameter value used in the numerical simulation are listed Table I. Here, injection level is defined as $(E_I / \tilde{E}_0)^2$, where E_I is the injected optical field amplitude just outside the SL facet and \tilde{E}_0 is the output optical field amplitude of the free-running SL. Outside the symmetric solid lines, no stationary solutions exist and the laser shows a beat phenomena. L/U means the periodic locking / un-locking region. For a detuning within symmetric solid lines, locking phenomena can be occurred. In ILIP region, which means injected light-induced pulsations, the SL exhibits the unstable locking characteristics such as pulsation close to the resonance frequency of the free-running laser, as mentioned above.

The SL transient responses under different locking conditions found in Fig. 2-1 can be solved by the fourth order Runge-Kutta integration of the rate equation. The laser spectra can be obtained from the fast Fourier transform of the SL output power at the steady-state solution of the transient response. In the calculations, noises are not taken into account. The dynamic solutions of

Table I. Laser Parameter and Their Numerical Values [13]

Symbol	Parameter	Value
t_s	Spontaneous emission lifetime	2ns
t_p	Photon lifetime	2ps
f_d	Longitudinal mode spacing	125 GHz
G_N	Gain coefficient	$1.1 \times 10^{-12} \text{ m}^3 \text{ s}^{-1}$
N_0	Carrier density to reach zero gain	$1.1 \times 10^{24} \text{ m}^{-3}$
α	Linewidth enhancement factor	3
I/I_{th}	Normalized bias current	1.3

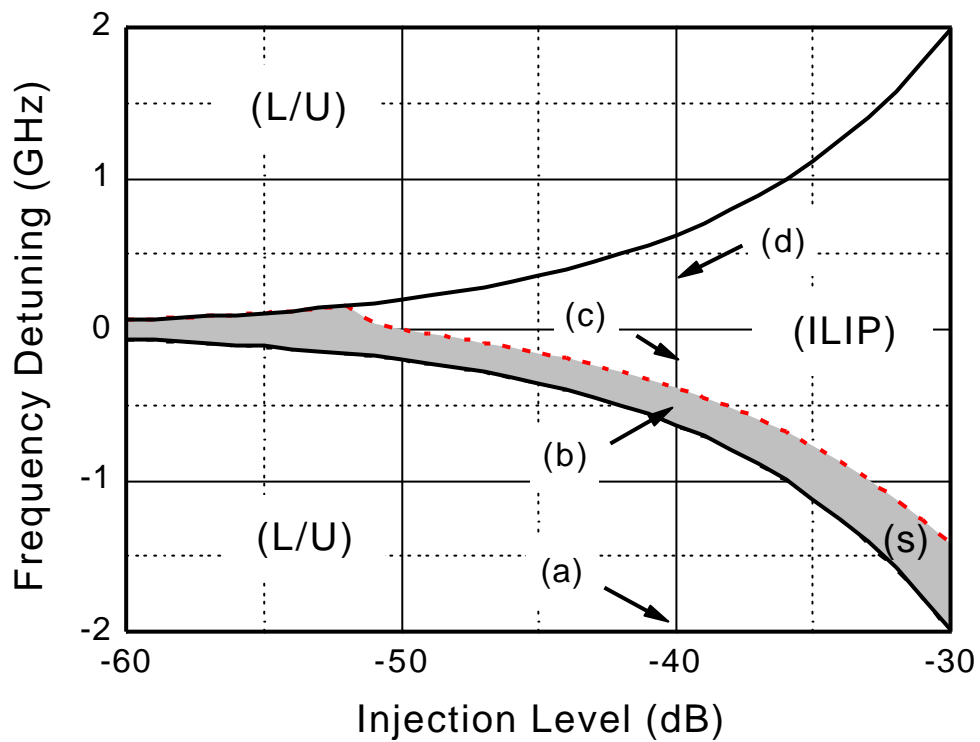
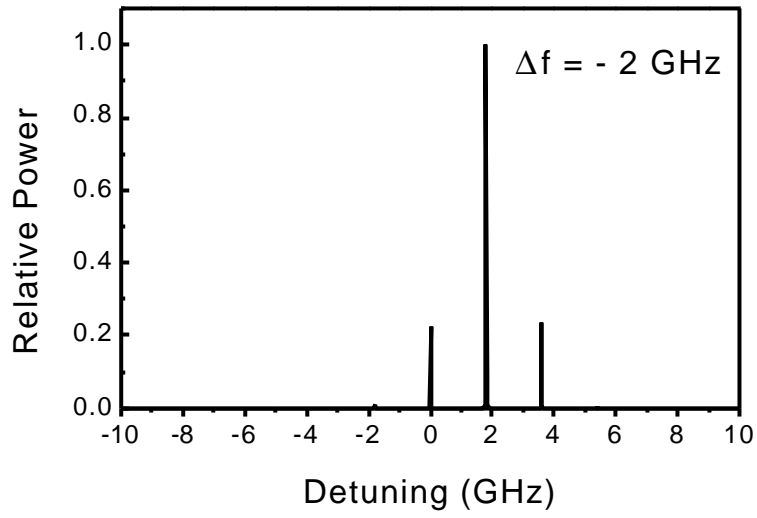


Figure 2-1. Characteristics of locking regimes as a function of injection level.

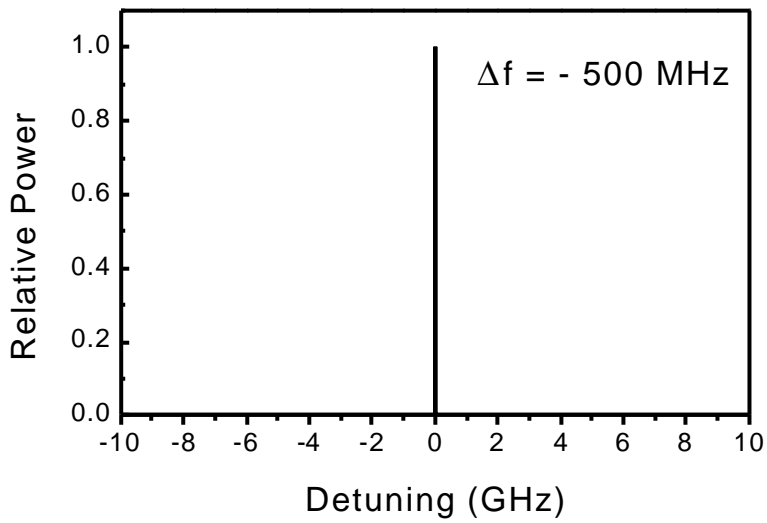
They are characterized into three regimes – L/U, ILIP, S – with different locking behaviors. L/U means the periodic locking / unlocking region, ILIP the injected light-induced pulsations and S the stable locking range. The filled area is the dynamically stable region.

the rate equation 3(a) – 3(c) depend strongly on the frequency detuning for a given injection level. Outside the locking range (the L/U region) the power switches between a locked and unlocked state in a periodic manner. In the dynamically unstable region (the ILIP region), the laser pulsates with a relaxation resonance frequency of several gigahertz. On the other hand, in the dynamically stable locking range (the S region), the laser is in a stable locked state and the output power of the injection-locked SL laser is centralized at a frequency of the ML.

Fig. 2-2 shows an example of calculated power spectra for a given injected level of -40 dB and different detuning values as marked in Fig. 1-1 as (a) – (d). In Fig. 2-2(a), the frequency detuning Δf is -2 GHz, which is located far from locking region. A large portion of the SL output power is located at a free-running SL's lasing frequency, and beat phenomena are noticed on the other side of the dominant power. The interaction between the ML and SL reduces the frequency difference, so the SL's lasing frequency becomes slightly closed to the MLs'. Fig. 2-2(b) with $\Delta f = -500$ MHz shows a stable locked state with all of the power concentrated at the ML frequency. In Fig. 2-2(c), the spectrum contains harmonics of the relaxation resonance frequency of 2.5 GHz. The situation in Fig 2-2(d) may be characterized as dynamically unstable locked states as in the Fig. 2-2(c), but the instability is too strong to maintain even a poor locking and a resultant spectrum shows many sidebands due to the unstable beat phenomena. From the analysis of injection locking characteristics, nonlinear distortion suppression by injection-locked semiconductor laser will be discussed in the following subsection.

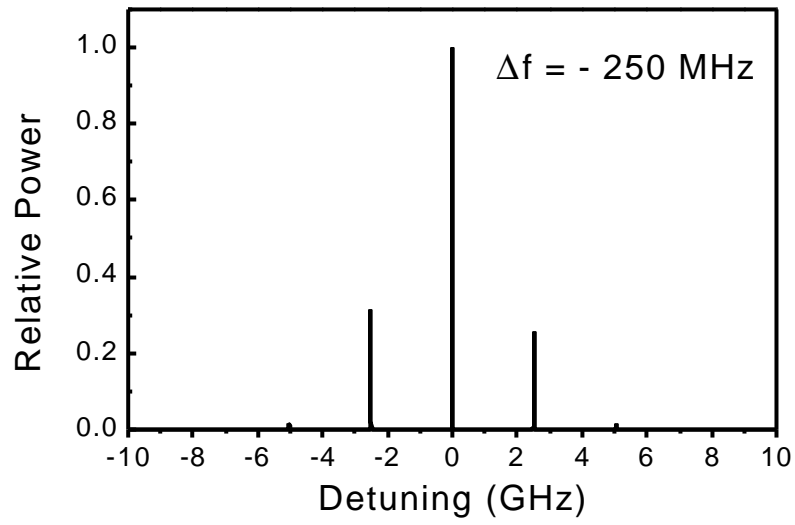


(a)

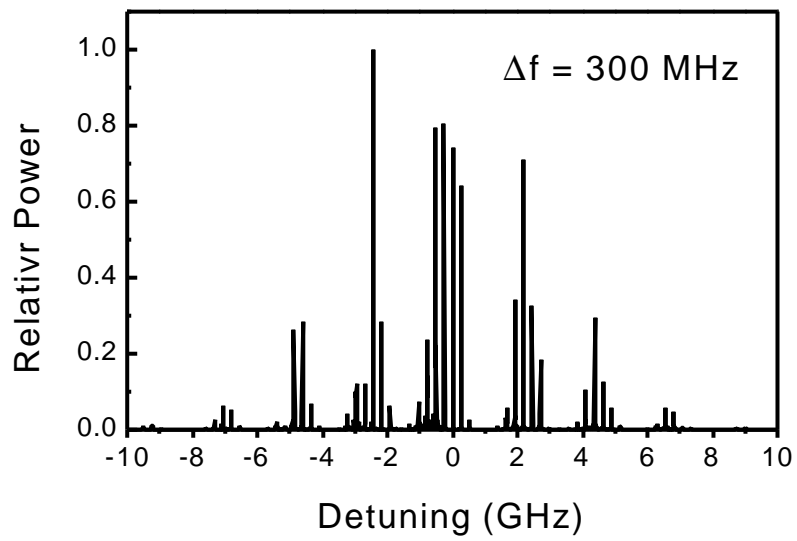


(b)

Figure 2-2. Power spectra for the different locking conditions, marked (a) ~ (d) in Fig. 2-1. The injection level is -40 dB.



(c)



(d)

Figure 2-2. (continued)

B. Nonlinear Distortion Suppression in Injection-locked DFB-LD

The optical analog transmission of GHz-range signals is recently attracting much interest for WLL (wireless local loop), CATV, and satellite system applications. In these applications, direct modulation of a semiconductor laser diode is used for transmitting signals multiplexed by RF-range subcarriers. Consequently, semiconductor laser nonlinearity becomes a crucial issue in the system performance because it can cause signal distortions by inter-channel interference, which limit the number of channels as well as transmission distance [8,15]. In low-frequency applications, such as CATV systems (< 1GHz), the distortion is mainly due to the nonlinear light-versus-current characteristic (L-I). In contrast, for high frequency SCM systems, such as cellular mobile communication systems, which operate in a multigigahertz range near the relaxation resonance frequency of semiconductor lasers, the nonlinearity induced by the coupling between photons and electrons in the laser cavity becomes dominant [16-18]. To suppress the nonlinearities of semiconductor lasers, injection locking has been extensively studied and experimentally confirmed [9]. In this subsection, the effects of optical injection locking on the nonlinear distortions of directly modulated DFB-LD are investigated by numerical simulations.

The nonlinear distortions induced by laser source nonlinearities can be numerically analyzed by the large signal analysis of the rate equations describing injection- locked SL [19];

$$\frac{dP(t)}{dt} = \Gamma G(N(t) - N_0)P(t) - \frac{P(t)}{t_p} + \frac{\mathbf{b} \Gamma N(t)}{t_n} + \frac{v_g}{L_c} (P(t) \cdot P_{inj})^{1/2} \cdot \cos(\Phi_{inj} - \Phi(t)) \quad 5(a)$$

$$\frac{dN(t)}{dt} = \frac{I(t)}{qV_a} - G(N(t) - N_0)P(t) - \frac{N(t)}{t_n} \quad 5(b)$$

$$\frac{d\Phi(t)}{dt} = \frac{1}{2} a \left\{ \Gamma v_g G(N(t) - N_0) - \frac{1}{t_p} \right\} - 2\mathbf{p}\Delta f + \frac{v_g}{2L_c} \left(\frac{P_{inj}}{P(t)} \right)^{1/2} \cdot \sin(\Phi_{inj} - \Phi(t)) \quad 5(c)$$

$$G = v_g a_0 / (1 + \mathbf{e}P(t)) \quad 5(d)$$

In the above, $P(t)$ and $N(t)$ are the photon and electron densities of the SL, $\Phi(t)$ is optical phase of the SL, Γ optical confinement factor, N_0 transparent carrier density, t_p photon lifetime, \mathbf{b} spontaneous emission factor, t_n carrier lifetime, v_g group velocity, a linewidth enhancement factor, a_0 gain coefficient, and L_c active layer cavity length. Δf and P_{inj} are lasing frequency difference between the ML and SL, and photon density injected into the SL's cavity. Φ_{inj} is set zero without loss of generality [10]. The locking behavior of semiconductor lasers strongly depends on two parameters; -injection ratio (R) and frequency detuning (Δf). The injection ratio is defined as the power ratio of the injected signal from the ML to the free-running SL output signal. The frequency detuning is the lasing frequency difference between the ML and free-running SL. Through the small-signal analysis of the rate equation 5(a) – 5(d), modulation responses against modulation frequency for the free-running and injection-locked lasers can be obtained. Fig. 2-3 shows the calculated frequency response of the DFB-LD. In this calculation, all parameter values are obtained from Table II and the output power of the SL is biased at 46 mA ($\cong 2 \times I_{th}$). The resonance peak of the laser with injection locking ($R = -5$ dB, $\Delta f = -12$ GHz) is considerably enhanced up to 11.7 GHz from the free-running

Table II. Laser Parameter Value for IMD3 Analysis [19]

Symbol	Parameter	Value
Γ	Optical confinement factor	0.2
N_0	Transparent carrier density	$1.0 \times 10^{18} \text{ cm}^{-3}$
t_p	Photon lifetime	0.9 ps
t_n	Carrier lifetime	1 ns
b	Spontaneous emission factor	1.0×10^{-4}
α	Linewidth enhancement factor	5
a_0	Gain coefficient	$3.17 \times 10^{-16} \text{ cm}^{-2}$
v_g	Group velocity	$7.5 \times 10^9 \text{ cm/s}$
V_a	Active layer volume	$45 \text{ } \mu\text{m}^3$

value of 3 GHz. Fig. 2-3 shows clearly that the modulation bandwidth can be enhanced with increasing injection ratio R .

It is known that the nonlinear distortion becomes more severe as the modulating frequency approaches the relaxation oscillation frequency due to the nonlinear coupling between electrons and photons. Hence, if the relaxation oscillation frequency of the laser is increased, the nonlinear distortions in multigigahertz range can be reduced. For narrow-band applications, the IMD3 of the closely spaced subcarriers is most important because the unwanted signals fall close to the original subcarriers. To observe the IMD3 due to the laser nonlinearities and its reduction by optical injection locking, semiconductor laser is modulated by two-tone RF signal ($f_1 = 2.6$ GHz, $f_2 = 2.7$ GHz). It can be numerically simulated using the rate equation by injecting two sinusoidal signals imposed on the bias current into the SL. SCM optical signal emitted from the SL is converted into complex electric field, and the obtained complex field is converted into detected RF signal using fast Fourier transform.

Fig. 2-4 shows the calculated results of the RF spectrum for the free-running and injection-locked lasers modulated by a two-tone RF signal. The power of each RF signal is kept at 0 dBm for both cases. To achieve the stable injection-locked state, the frequency detuning Δf is -12 GHz, where frequency detuning for the stable injection-locked state ranges from -3.7 GHz to -42.9 GHz at the injection ratio $R = -5$ dB. The IMD3 defined as the ratio of the power at third-order intermodulation product (IMP3) frequency to the power at the fundamental modulating frequency. As shown in Fig 2-4(a), IMD3 for free-running laser is -36 dBc. On the other hand, Fig. 2-4(b) shows the

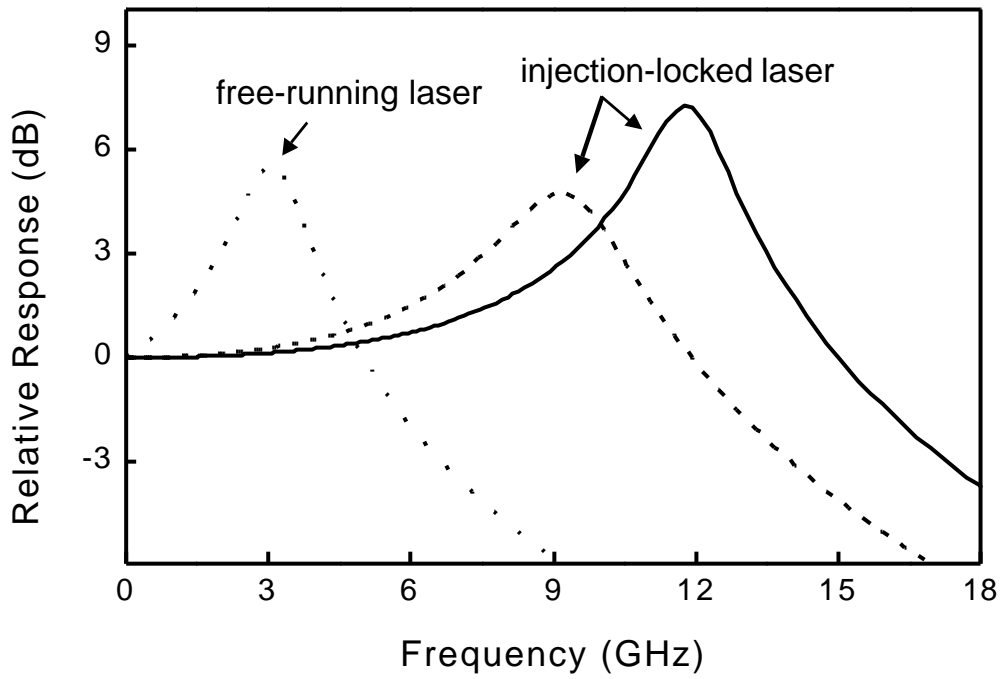
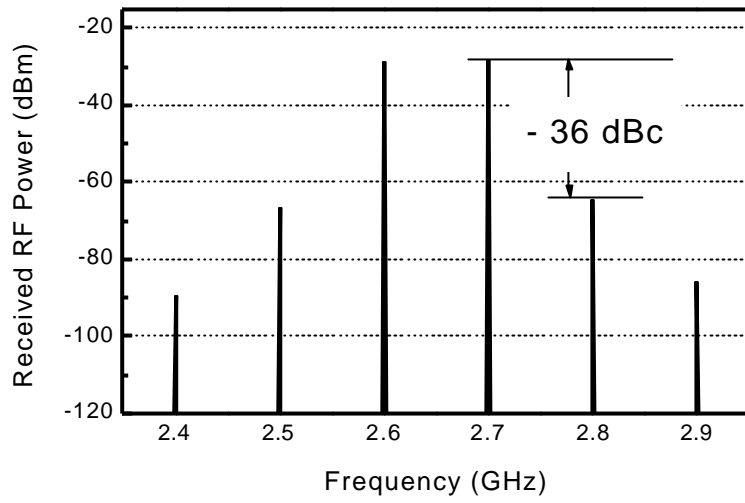


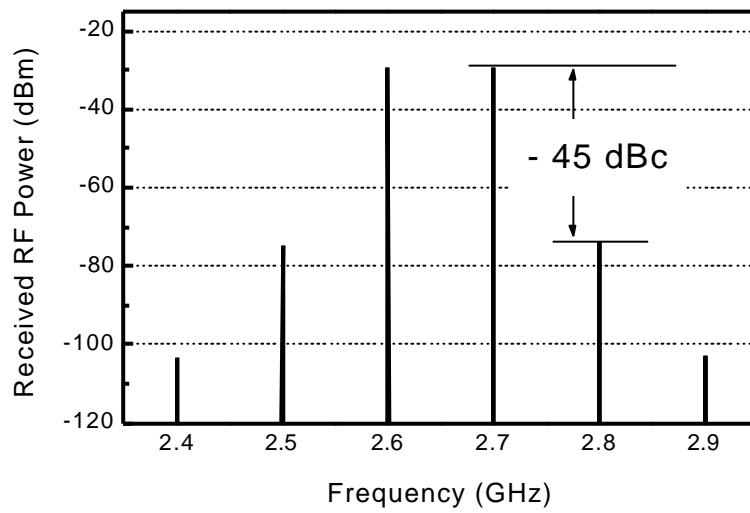
Figure 2-3. Frequency responses both the free-running and injection-locked lasers.

----- injection power ratio -10 dB, frequency detuning -10 GHz

———— injection power ratio -5 dB, frequency detuning -12 GHz



(a)



(b)

Figure 2-4. Simulated RF Power spectra of the DFB-LD by a two-tone RF signal($f_1 = 2.6$ GHz, $f_2 = 2.7$ GHz). for the free-running (a) and injection-locked lasers (b).

corresponding power spectrum for the DFB-LD under injection locking. The IMD3 is considerably reduced by -45 dBc. In addition, the fifth-order intermodulation products located at 2.4 GHz ($3f_1 - f_2$) and 2.9 GHz ($3f_2 - f_1$) can be also reduced by about 20 dB by employing optical injection locking technique.

Fig. 2-5 shows the received RF powers of the fundamental and IMP3 against the input RF power for both free-running and injection-locked lasers. With the optical injection locking, the spurious-free dynamic range (SFDR) can be improved from 53 dB \cdot MHz^{2/3} to 56.5 dB \cdot MHz^{2/3}. Consequently, by the rate equation analysis with the optical injection term, it is found that the IMD3 of the injection-locked DFB-LD can be much reduced due to the relaxation oscillation frequency increase and the resulting SFDR is also increased. In section III and section IV, the experimental observation of IMD3 reduction by optical injection locking of FP-LD and the IMD3 variances over the fiber transmission is discussed experimentally.

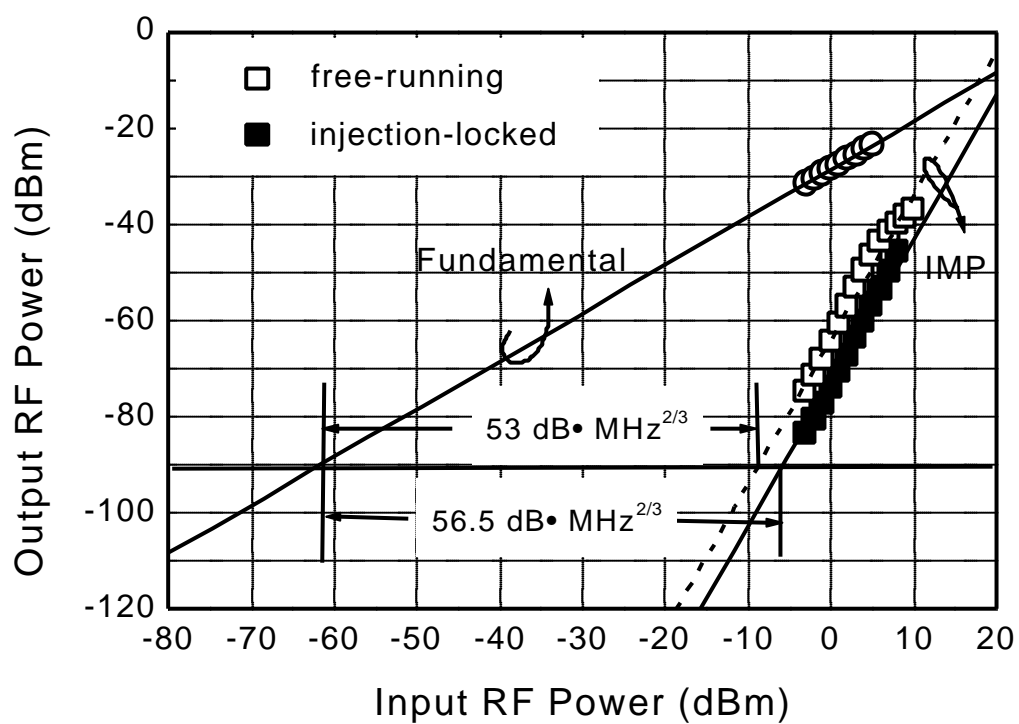


Figure 2-5. The SFDR of the link with directly modulated DFB-LD for the free-running and injection-locked laser.

III. IMD3 Reduction of Injection-locked FP-LD

The modulation bandwidth of semiconductor lasers is approximately proportional to the relaxation oscillation frequency. Therefore, much effort has been made to increase the relaxation oscillation frequency. In many approaches to increase the relaxation oscillation frequency and suppress the nonlinearities of the semiconductor lasers, injection-locking technique of DFB-LD has already been analyzed in the previous section. In this section, we examine the injection locking bandwidth and make the first experimental demonstration of the IMD3 suppression at the different injection target modes of FP-LD.

A. Injection-locking Bandwidth of FP-LD

Injection locking characteristics of an intermodal injection-locked Fabry-Perot semiconductor lasers were reported theoretically by J. M. Luo et al. [22] and experimentally by Y. Hong et al. [23]. They showed that at a fixed optical injection power, the relaxation oscillation frequency increases when light is injected into a shorter wavelength mode and a larger stable locking range is achieved by choosing an appropriate injection target mode.

For the measurement of the stable locking ranges and the reduction of IMD3 at a different target mode of a FP-LD, the experimental setup is illustrated in Fig. 3-1. An external cavity tunable laser (TL) with a tuning range of 0.002nm is used as a ML and a commercially available FP-LD (SAMSUNG, SFL24-B1-3) with mode spacing of ~ 0.84 nm at a dc bias of

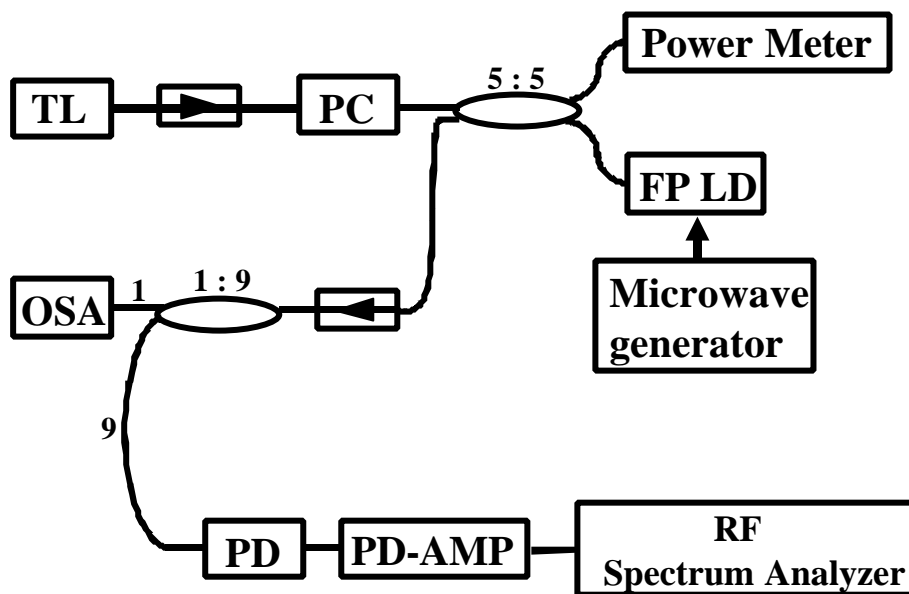
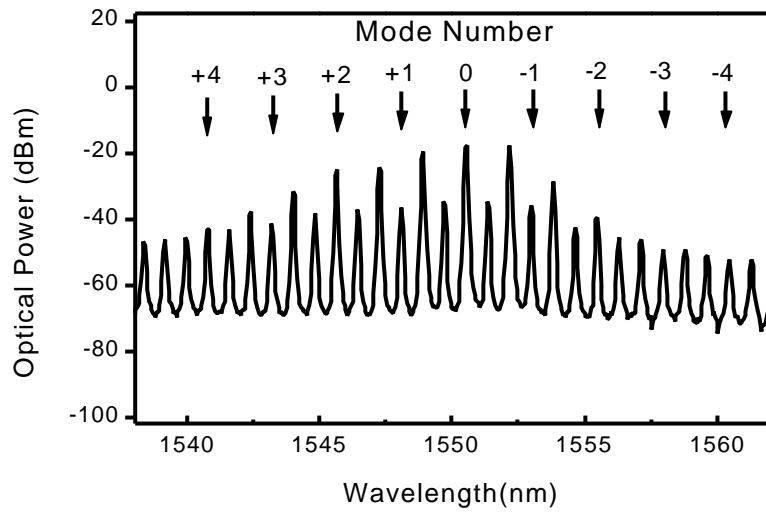


Figure 3-1. Experimental setup. PC : Polarization controller, TL : External cavity tunable laser, PD : Photodetector, OSA : Optical spectrum analyzer, PD- AMP : Photodetector Amplifier

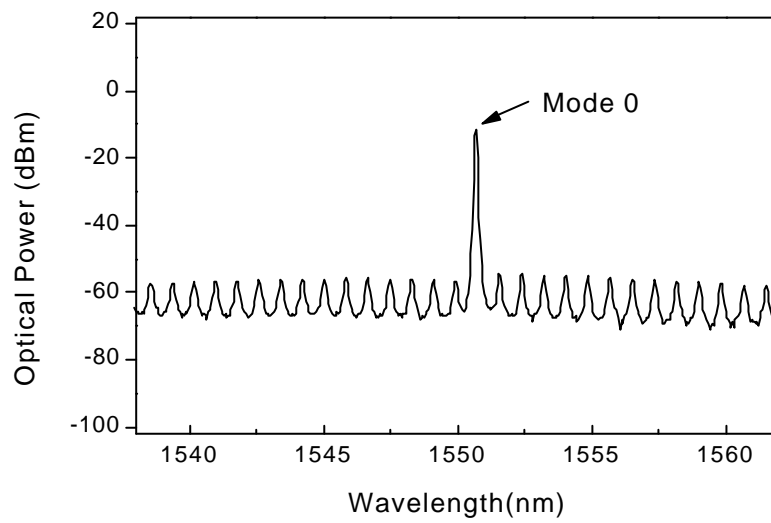
19.0mA is used as a SL. Two optical isolators of >50 dB isolation are used to prevent light coupling from the SL to the ML and to protect the ML against backreflected light. The optical spectrum analyzer and RF spectrum analyzer are used to monitor the stable injection-locked state.

Fig. 3-2(a) shows optical spectrum of free-running FP-LD and definition of mode number for the FD- LD operating at dc bias 19.0mA. Mode number 0 (wavelength = 1550.52 nm) is the peak of all FP-LD lasing modes, positive mode number indicates shorter wavelength than mode 0, and negative mode number indicates longer wavelength than mode 0. Each selected mode is spaced by 3 mode difference from defined neighboring modes. Fig. 3-2(b) shows that under stable strong injection at mode 0 from the ML, mode 0 is dominant and other modes are sufficiently suppressed at a degree of mode suppression ratio (MSR) >40 dB. Similarly, as shown in Fig. 3-2(c) and Fig. 3-2(d), injections at mode +4 and mode -4 also suppress of the other entire mode with almost the same MSR as in the mode 0 injection case.

Stable locking ranges at different injection target modes are determined by observing optical power spectra of OSA and beat phenomena of RF spectrum analyzer. The measured stable locking bandwidth at 9 different injection target modes varying injecting power is shown Fig. 3-3. The frequency detuning is defined the difference of the ML's frequency and SL's free running target mode frequency. In accordance with the known result that injection locking bandwidth increases as the injection ratio increase [23], the stable injection locking bandwidth becomes larger as the increase of the TL injection power. At the same TL injection power, the maximum injection locking bandwidth is achieved in a higher mode. The result for injection into positive modes is in



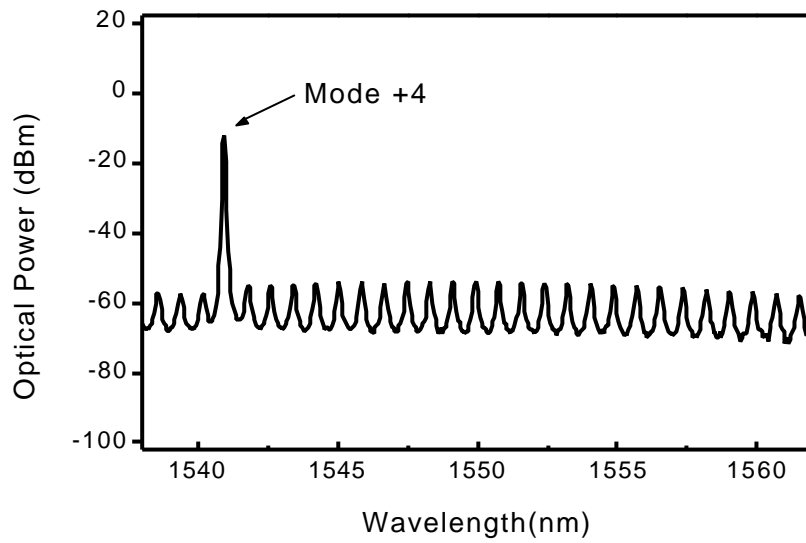
(a)



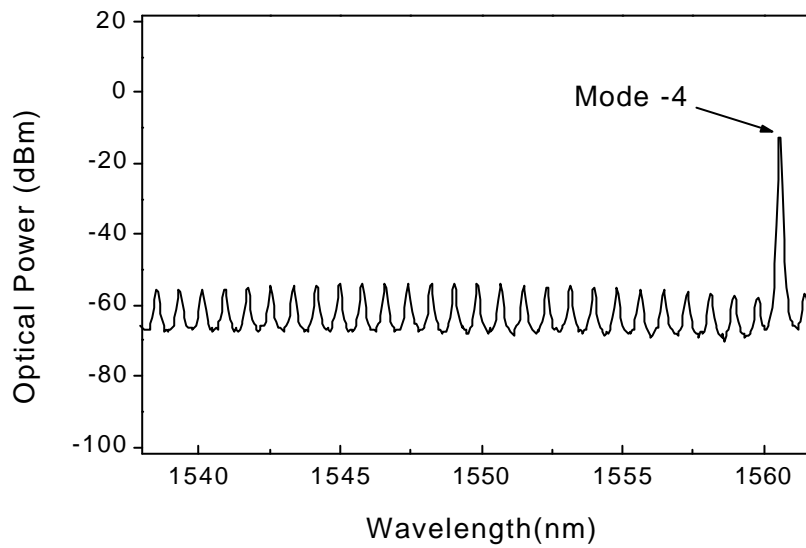
(b)

Figure 3-2. Optical power spectra of FP-LD and definition of mode number.

(a) free-running and (b) injection into 0 mode at 5 dBm ML output power



(c)



(d)

Figure 3-2. (continued)

(c) injection into +4 mode at a 5 dBm ML output power

(d) injection into -4 mode at a 5 dBm ML output power

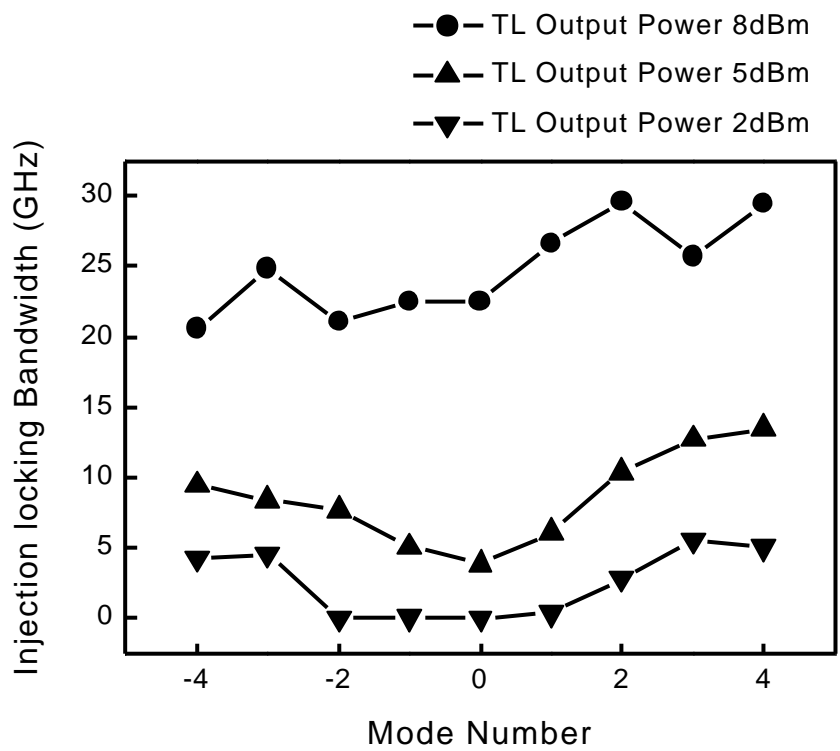


Figure 3-3. Injection locking bandwidth versus mode number.

TL output power is set at 2, 5, and 8 dBm, respectively.

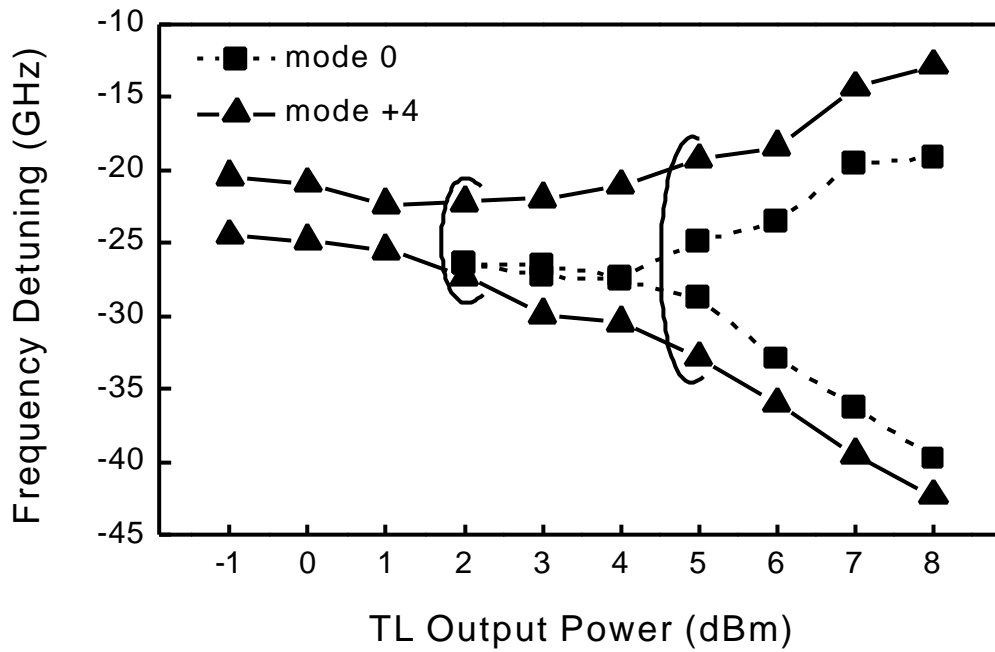


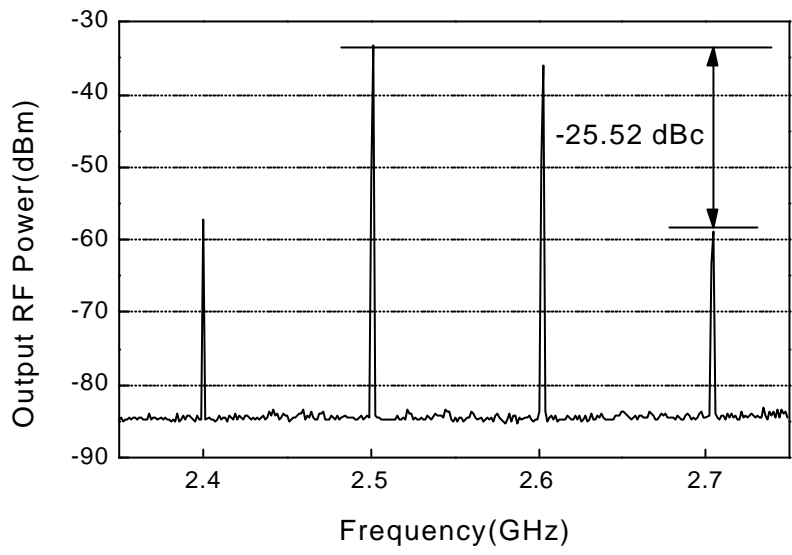
Figure 3-4. Frequency detuning versus the ML output power for injection target mode 0 and +4 respectively. For mode 0, below TL output power 2 dBm, frequency detuning is not distinguishable.

agreement with theoretical predictions [22]. At the TL output power 8 dBm, injection locking bandwidth ranges more than about 20 GHz in the entire different injection modes. Fig. 3-4 confirms the result because the injection locking bandwidth is larger at mode +4 injection than at mode 0 injection and becomes larger at stronger injection. As reported previously [22]-[23], the injection into short-wavelength target mode (positive mode number) increases the stable locking range and this characteristic is related to gain peak shifts towards longer wavelength and injection power ratio of the ML to SL's injection target mode at free running.

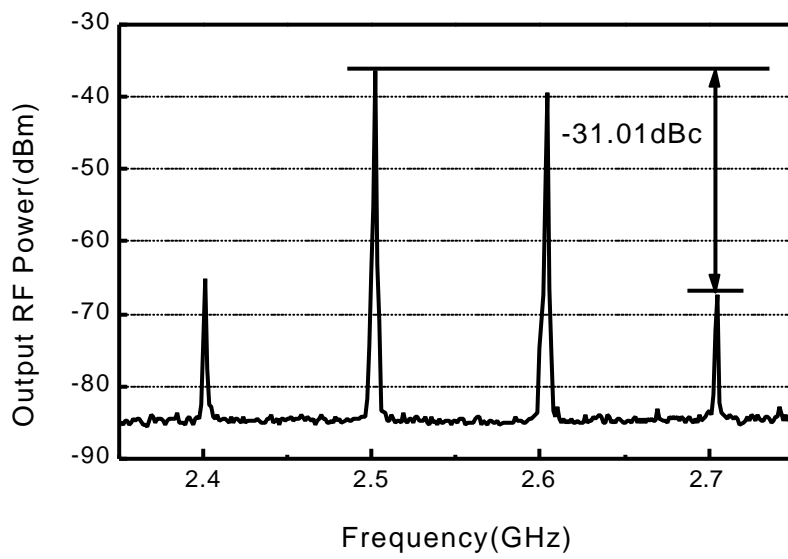
B. Dynamic Range Enhancement

The characteristics of IMD3 for different injection target modes under modulating the SL by two-tone RF signals ($f_1 = 2.5\text{GHz}$, $f_2 = 2.6\text{GHz}$) are investigated. For each of the selected injection target mode, the ML frequency is chosen at the center of each stable locking range. Fig. 3-5 shows measured RF spectra for the free-running and mode +4 injection-locked case because mode +4 has the largest injection locking bandwidth of 9 injection target modes and been expected to have the more increased relaxation oscillation frequency. In Fig. 3-5(a), the IMD3 is -25.52 dBc for free-running FP-LD. Fig. 3-5(b) shows the IMD3 of -31.01 dBc for mode +4 injection-locked case and significant suppression of IMD3 at the frequency of $2f_2 - f_1 (=2.7\text{GHz})$ and $2f_1 - f_2 (=2.4\text{GHz})$ compared to free-running case.

We only concern about the one IMD3, $2f_2 - f_1$ because two IMP3s have symmetric characteristic. Fig. 3-6 shows the power of fundamental



(a)

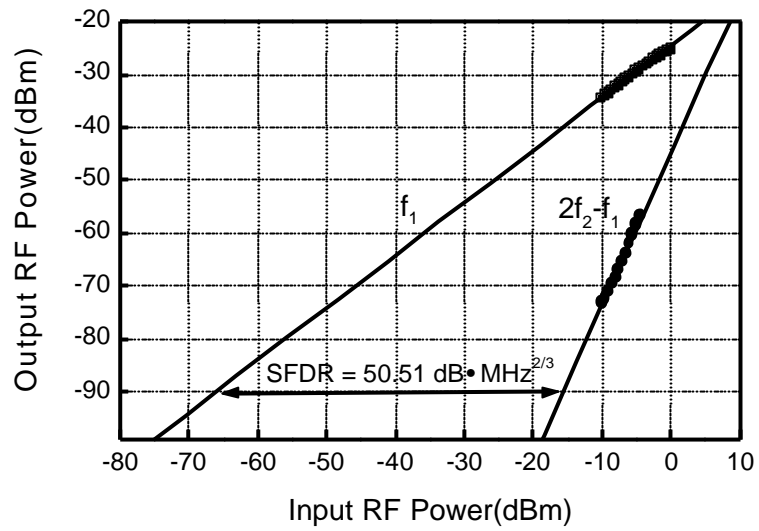


(b)

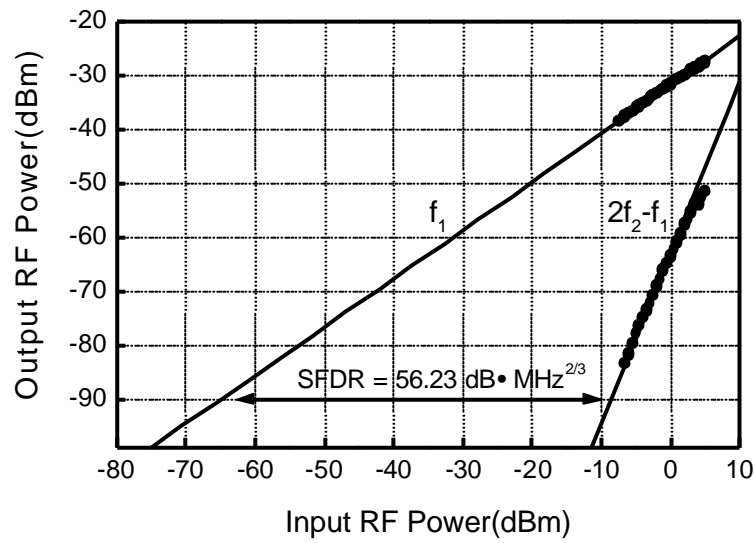
Figure 3-5. Measured RF spectra (a) free-running, (b) mode +4 injection locking, Two-tone RF power +4dBm, ML output power +5dBm.

components and IMP3 of FP-LD output as a function of modulating two-tone RF signal power where two-tone RF signal powers are the same. By linear fitting, spurious-free dynamic range (SFDR) can be estimated. Compared with the free running case, mode +4 injection-locked case shows reduction of IMD3. Consequently, SFDR is significantly enhanced at the latter case. Using the same experimental procedure, powers at the fundamental component and IMP3 are measured for 8 modes defined in Fig. 3-2(a). Fig. 3-7 shows normalized SFDR, which is defined as the ratio of SFDR in free-running case to injection-locked case. Injection locking into any sidemode reduces IMD3 compared to free running and choosing an appropriate injection target mode, especially positive mode number, significantly improves nonlinear suppression of FP-LD.

In this section, the nonlinear distortion suppression of FP-LD by optical injection locking has been experimentally investigated. The intermodal injection locking characteristics of FP-LD for 9 different target modes have been examined, and it has been showed that at a fixed injection power, injection into shorter wavelength from a peak mode is useful to enlarge stable locking range. For the injection-locked states into different injection target modes, experimental measurements of IMD3 reduction were also performed. It was showed for the first time that the IMD3 reductions are achievable at any target mode injection locking. Consequently, choosing an appropriate injection target mode can enlarge stable locking bandwidth and reduce the IMD3 significantly.



(a)



(b)

Figure 3-6. Measured FP-LD output RF component and IMD3 versus modulating input RF power. (a) free-running and (b) mode +4 injection

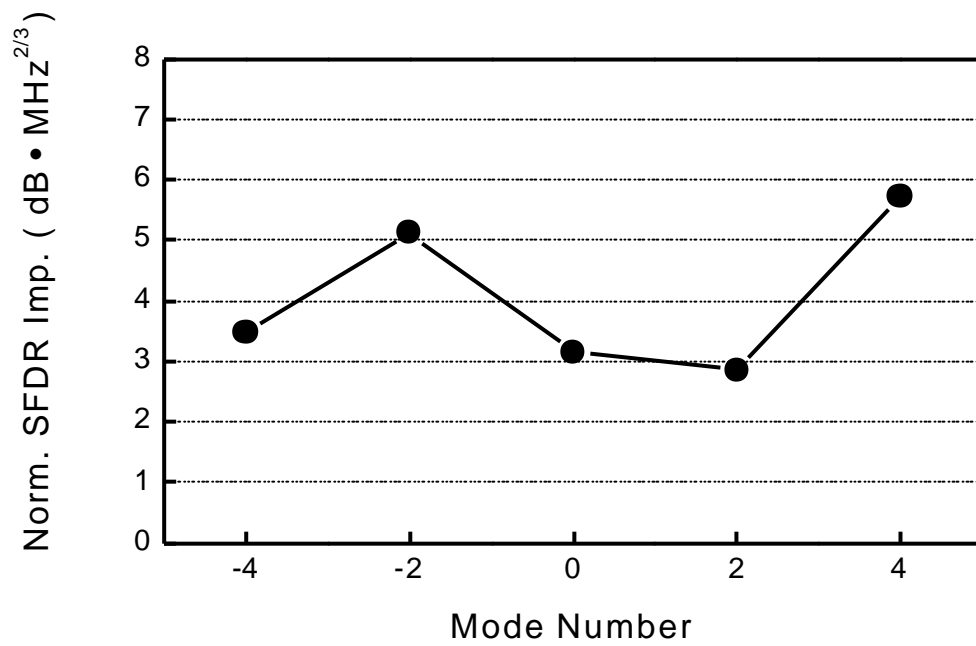


Figure 3-7. Normalized SFDR improvement for all injection target modes. The noise floors is assumed -90dBm .

VI. Dispersion-induced IMD3 over Fiber Transmission

In section II and III, IMD3 suppressions in injection-locked DFB-LD and FP-LD have been discussed. However, IMD3 variations over fiber transmission, when injection-locked semiconductor lasers are used, have not been studied yet. In this section, the fiber dispersion-induced IMD3 variations for the free-running and injection-locked DFB- / FP-LD are investigated numerically and experimentally. It is found that the dispersion-induced IMD3 increases during fiber transmission because of the combined effect of laser source nonlinearities and fiber chromatic dispersion, and it can be much reduced and less dependent on fiber transmission length by using injection-locked DFB- / FP-LD.

A. IMD3 for DFB-LD

A – 1. Experiments

Fig. 4-1 shows the experimental setup for measuring the IMD3 dependence on fiber length for free-running and injection-locked semiconductor lasers. The external-cavity tunable light source is used for a ML. For a SL, a commercially available, unisolated DFB-LD (Samsung SDL-24) is used. Optical circulator with >40dB isolation is used to prevent light coupling from the SL to the ML and protect the SL against backreflected light. For generating subcarriers, the SL is directly modulated with two-tone RF signals, of which frequency is $f_1 = 2.6$ GHz and $f_2 = 2.7$ GHz. The standard single-

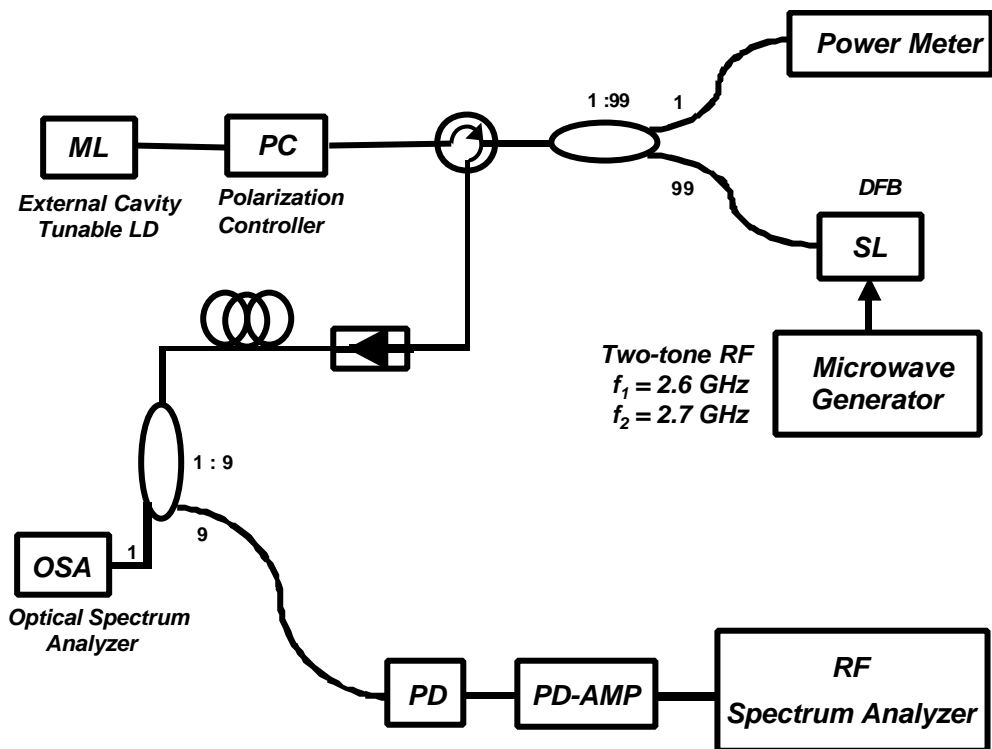


Figure 4-1. Experimental setup

mode fiber is used in the experiment.

For both free-running and injection-locked states, SL is biased at 15mA ($\cong 1.9 \times I_{th}$). Each power level of RF signals before Bias-T is set at -6dBm. To achieve the stable injection-locked state, the frequency difference between ML and SL is set at 10 GHz, where stable locking range about 20 GHz and the injection ratio at about -5 dB. Received RF powers at the fundamental ($f_2 = 2.7$ GHz) and IMP3 ($2f_2 - f_1 = 2.8$ GHz) frequencies are measured while the fiber length is varied in the increment of 5 km up to 40 km.

Fig. 4-2 shows the measured RF spectra at the fundamental and IMP3 frequencies in the free-running state. The dispersion-induced IMD3 is, here, defined as the ratio of the power at third-order intermodulation product (IMP3) frequency to the power at the fundamental modulating frequency. The IMD3 for the free-running state is -21.5 dBc at 0km and increases to -11.0 dBc at 30km as shown in Fig. 4-2(a) and 4-2(b), respectively. The reduced power at fundamental frequency after 30km transmission is mainly due to fiber loss ($\cong -0.2$ dB/km), but the power at IMP3 frequency is not reduced so much due to fiber dispersion. The IMD3 after 30km transmission is increased by 10.5 dB. For the injection-locked state (Fig. 4-3(a), (b)), IMD3 is -27.17 dBc at 0 km and -26.0 dBc at 30 km. In this case, IMD3 increase is only 1.17 dB and about 15dB reduction in IMD3 compared to free-running DFB-LD are achieved by using injection-locked DFB-LD.

The reduction of fiber dispersion-induced IMD3 for the injection-locked laser can be explained as follows. When semiconductor laser is directly modulated by RF signals, modulated optical spectra are broadened by intensity (IM) and frequency modulation (FM) effect. Harmonic and intermodulation

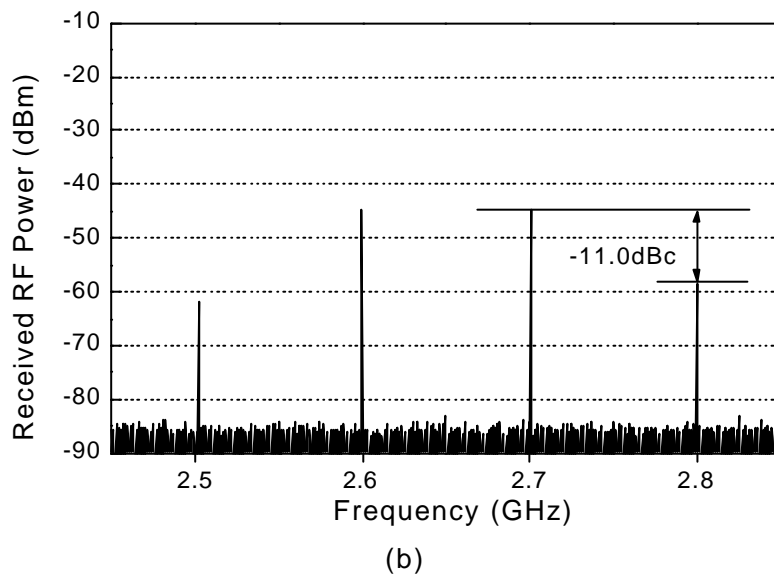
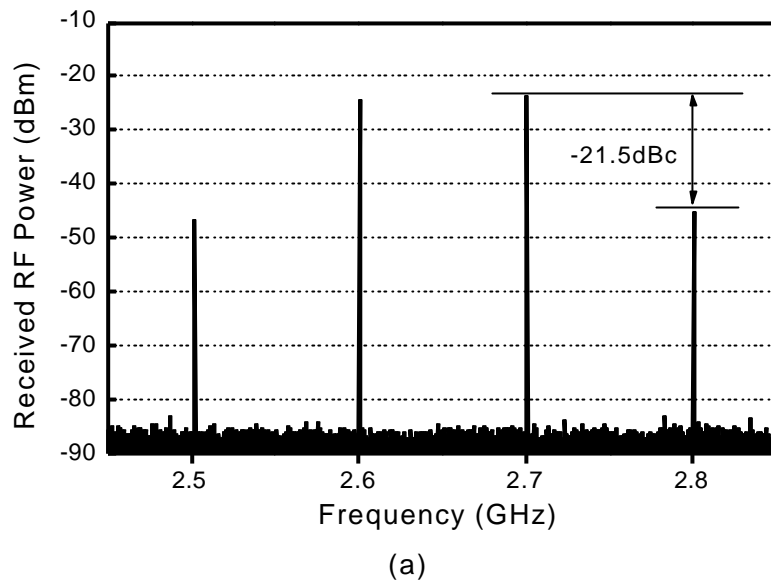


Figure 4-2. Measured RF power spectra for the free-running DFB-LD directly modulated by a two-tone RF signal ($f_1 = 2.6$ GHz, $f_2 = 2.7$ GHz).
 (a) 0km (b) 30km transmission

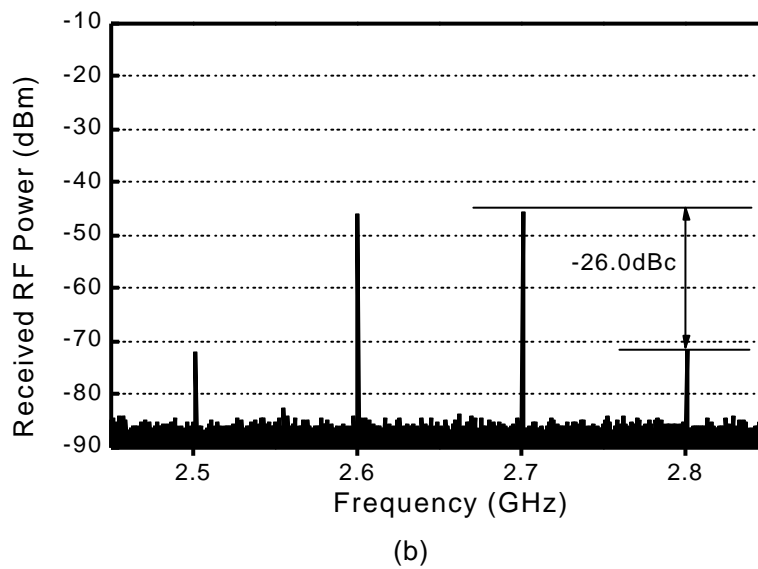
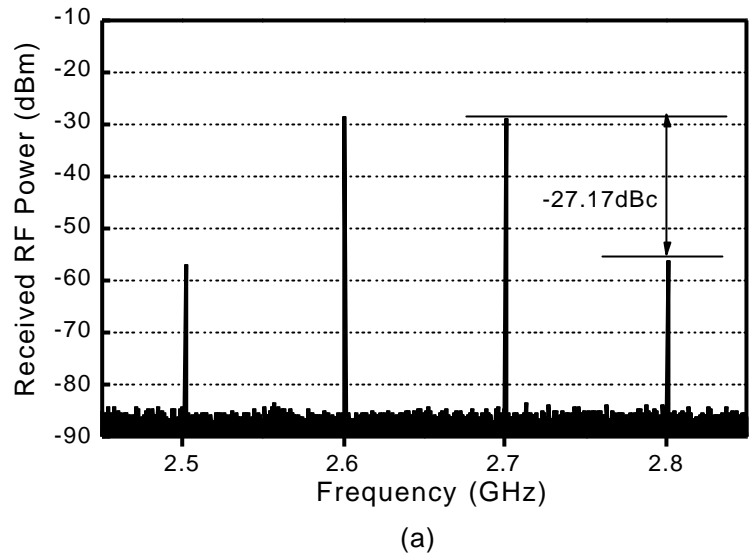


Figure 4-3. Measured RF power spectra for the injection-locked DFB-LD directly modulated by a two-tone RF signal ($f_1 = 2.6$ GHz, $f_2 = 2.7$ GHz). (a) 0km (b) 30km transmission

products are produced by these broadened optical spectra, and vary during transmission by fiber dispersion and loss [4]. Fig. 4-4 shows optical spectra measured by Fabry-Perot interferometer for the free-running and injection-locked DFB-LD directly modulated by a two-tone RF signal. Injection-locked DFB-LD has narrower optical spectrum than free-running DFB-LD due to reduced laser chirping.

In Fig. 4-5(a), the received RF powers at the fundamental and IMP3 frequencies are plotted for the free-running state at various fiber lengths. Overall, the received RF powers at both fundamental and IMP3 frequencies decrease with fiber length due to the fiber loss. The IMD3 increases during transmission due to fiber dispersion. IMD3 variations on fiber length are shown in Fig. 4-5(b). The IMD3 is -21.5dBc back-to-back and -9.31dBc at 40km transmission, which shows IMD3 degradation of 12.19dB after 40km transmission. However, for the injection-locked state (Fig. 4-6(a)), powers at fundamental and IMP3 frequencies decrease almost at the same rate. Due to the enhanced laser linearities such as frequency chirp reduction, IMP3 also decreases at the same rate as fundamental power decrease. As shown in Fig. 4-6(a), in the injection-locked state, IMD3 is -27.17dBc back-to-back and -25.62dBc at 40km transmission. The IMD3 degradation is only 1.55dB in the injection-locked state and its variation is maintained within about 2dB for the entire transmission length. Compared to the free-running state, in the injection-locked state, 16.3dB reduction in IMD3 is achieved for 40km fiber transmission.

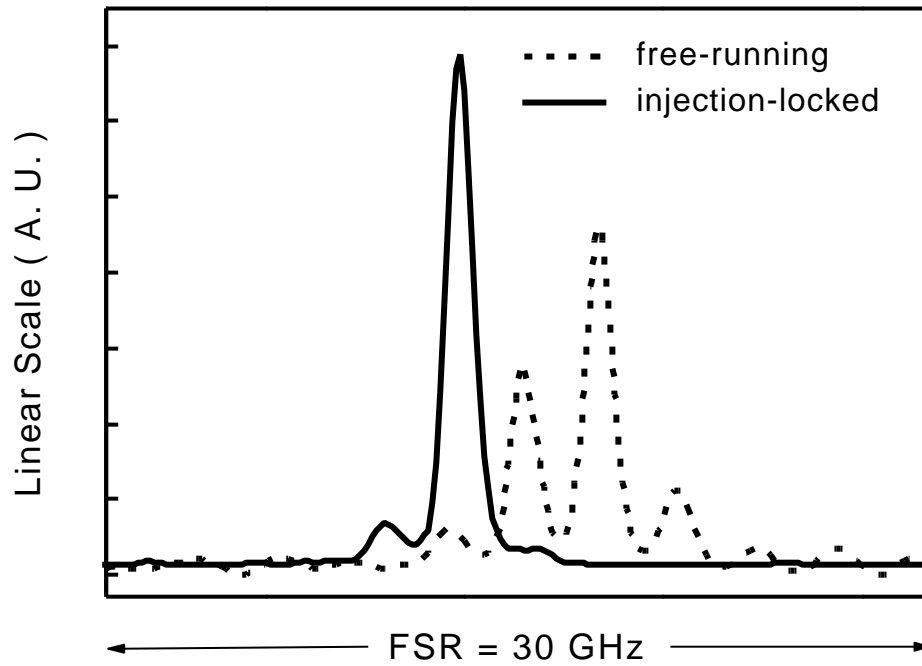
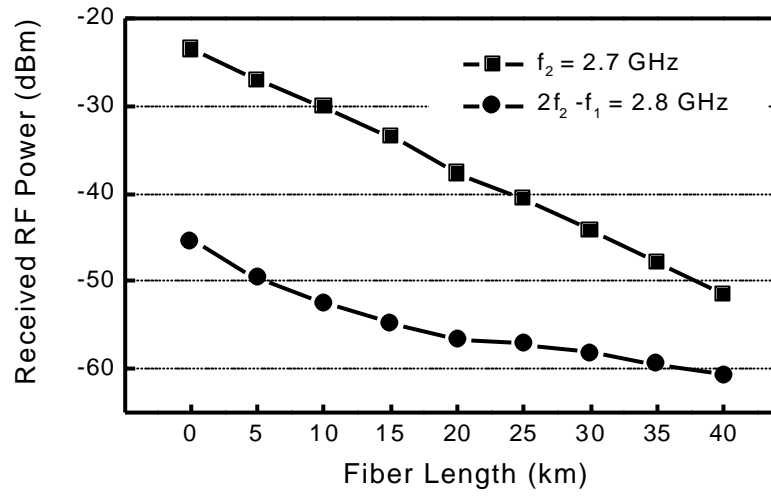
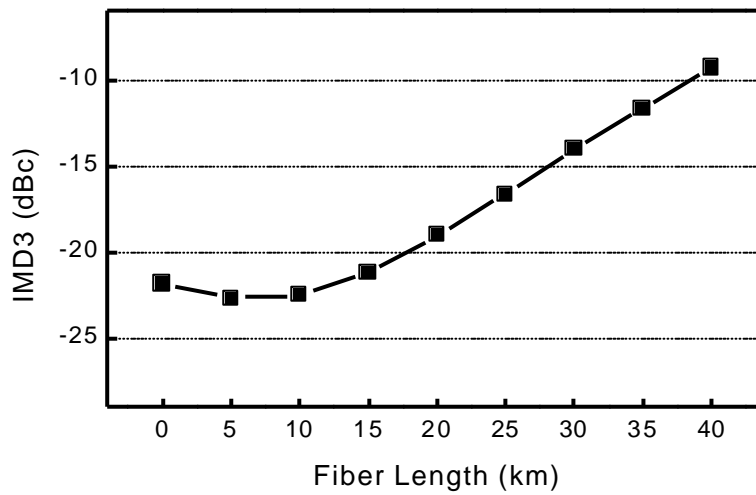


Figure 44. Optical spectra measured by Fabry-Perot interferometer for the free-running and injection-locked DFB-LD directly modulaed by a two-tone RF signal ($f_1 = 2.6$ GHz, $f_2 = 2.7$ GHz)

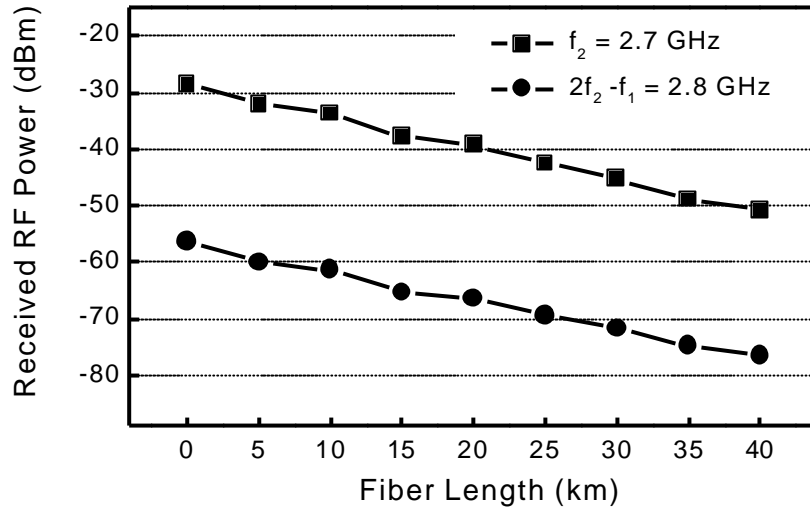


(a)

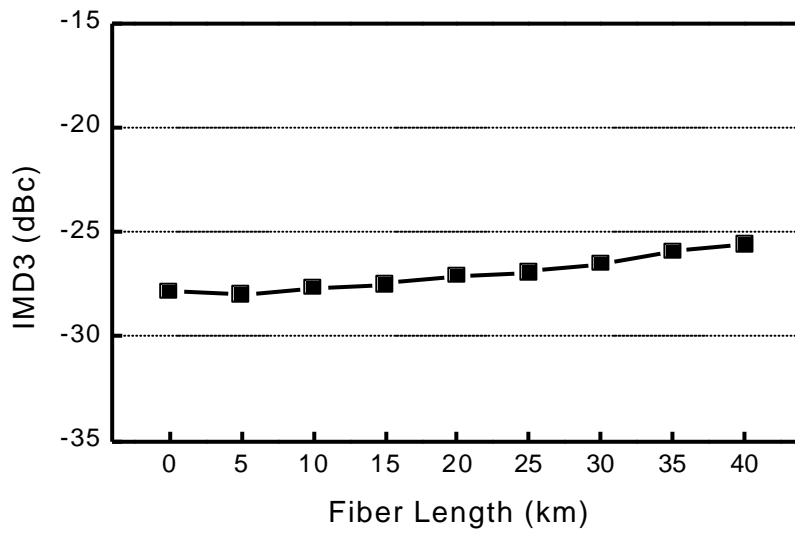


(b)

Figure 4-5. (a) Received RF power at f_2 and $2f_2 - f_1$ versus fiber length
 (b) IMD3 versus fiber length for the free-running state.



(a)



(b)

Figure 4-6. (a) Received RF power at f_2 and $2f_2 - f_1$ versus fiber length
 (b) IMD3 versus fiber length for the injection-locked state.

A - 2. Simulations

The IMD3 induced by laser source nonlinearities can be numerically analyzed by the large signal analysis of the rate equations 5(a) - 5(d) describing injection-locked SL [19]. The SL direct modulation is obtained by

$$I(t) = I_{bias} + \sum_k I_k \cos(2\pi f_k t) \quad (6)$$

modulating injection current $I(t)$, where I_{bias} is bias current for SL, I_k is the amplitude of k th subcarrier, and f_k is the modulating frequency of k th subcarrier. In order to consider the effect of the fiber chromatic dispersion combined with laser source nonlinearities, SCM optical signal emitted from the SL is converted into complex electric field and the obtained complex field transmits through dispersive fiber. The dispersive fiber is linearly modeled as [24],

$$H(f) = \exp\left(\frac{j\pi D L f^2}{c}\right) \quad (6)$$

where λ is wavelength of CW laser, D fiber dispersion coefficient, L fiber length, and c speed of light in free space. Fig. 47(a) shows the calculated results of IMD3 at the different modulation index and fiber length for the free-running state under no light injection. Two-tone modulating RF frequency is $f_1 = 2.6$ GHz and $f_2 = 2.7$ GHz. Intensity modulation (IM) index m_I is defined as $m_I = I_k / (I_{bias} - I_{th})$, where I_{th} is the threshold current of the semiconductor laser. In the free-running state, IMD3 becomes larger with the increase of either fiber transmission length or IM index due to combined effect of laser nonlinearity and fiber chromatic dispersion. When the semiconductor laser is injection locked, semiconductor laser frequency chirp dominating frequency modulation (FM) index and degrading the system performances combined

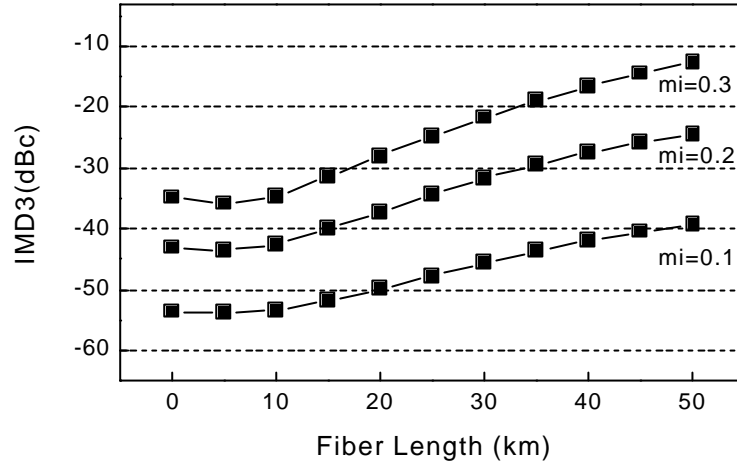
with fiber dispersion [8], can be significantly reduced. Because of the FM index decrease, fiber dispersion-induced IMD3 of the injection-locked DFB-LD is not degraded over fiber transmission, as shown in Fig. 4-7(b), and, at no transmission, IMD3 is much suppressed compared to the free-running state [9].

B. IMD3 for FP-LD

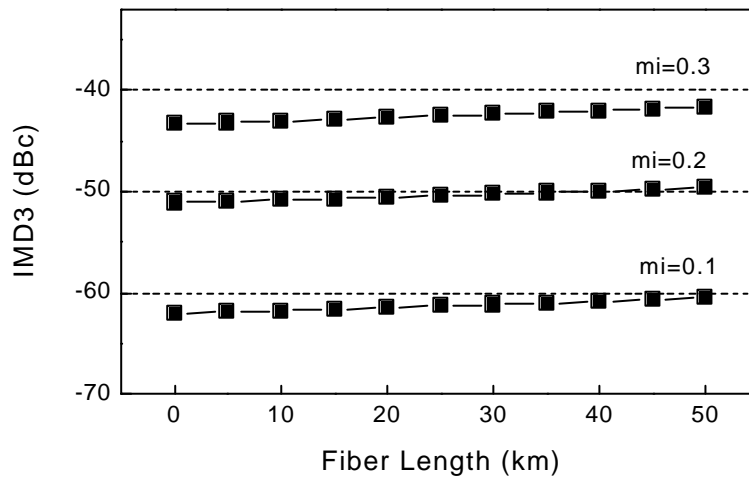
FP-LD is used as a SL instead of DFB-LD in order to investigate the IMD3 dependence of FP-LD on fiber length in the experimental setup shown Fig. 4-1. The SL is again biased at 15mA ($\cong 3.3 \times I_{th}$) and directly modulated by two-tone RF signals at $f_1 = 2.6$ GHz and $f_2 = 2.7$ GHz. The power level of both RF signals before Bias-T are kept at -6 dBm. In order to achieve stable injection locking, one injection target mode among FP-LD's multi-modes is chosen and the ML is tuned within the locking bandwidth. In this experiment, we chose a sidemode located at the shorter wavelength side from the peak mode so that the larger injection locking bandwidth can be utilized [23]. Since the optical power of the injection-locked FP mode is much smaller compared to that of DFB-LD's fundamental mode, the injection locking bandwidth is much larger for FP-LD than DFB-LD. Hence, the injection locking of FP-LD can be achieved more easily than DFB-LD. The injection ratio between ML and FP-LD target mode is about 0 dB and the stable locking range is about 40 GHz.

Fig. 4-8 shows the measured RF spectra at the fundamental and IMP3 frequencies in the free-running state when the FP-LD is used as the SL. The IMD3 for the free-running state is -19.3 dBc at 0km and increases to -0.9 dBc at 20km as shown in Fig. 4-8(a) and 4-8(b), respectively. The IMD3 after

20km transmission is increased by 18.4 dB. For the injection-locked state (Fig.



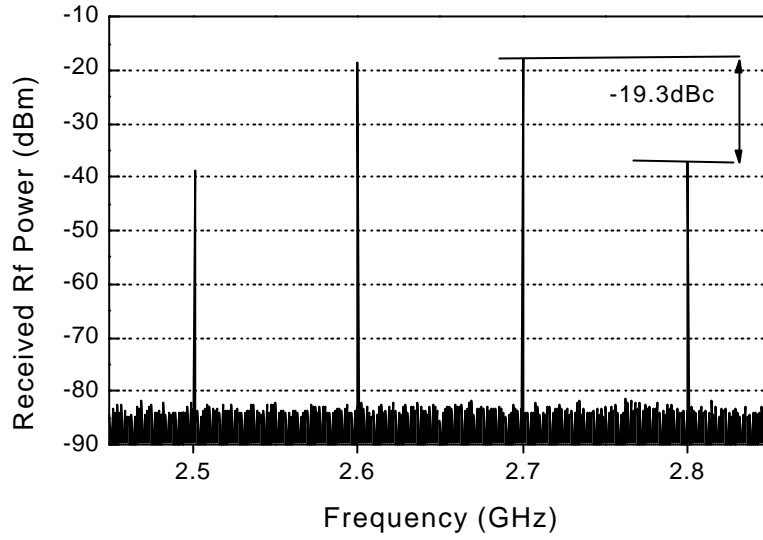
(a)



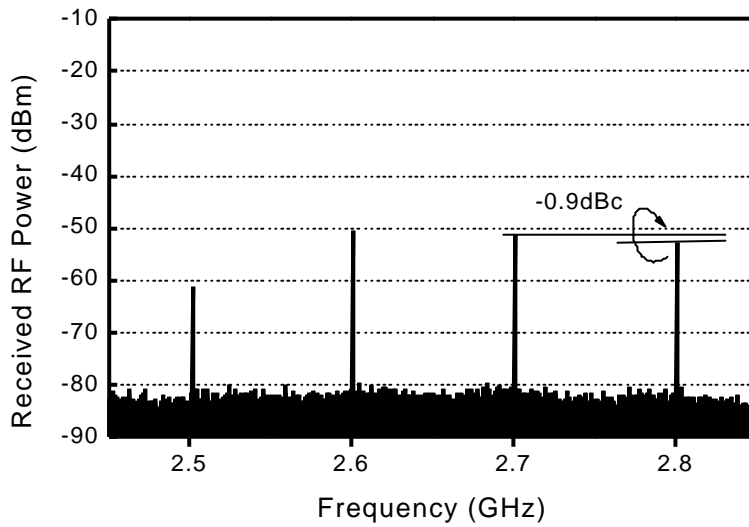
(b)

Figure 47. Numerical Simulation of fiber distortion-induced IMD3 for (a) free-running, and (b) injection-locked DFB-LD. For the injection-locked DFB-LD, frequency detuning Δf is -13GHz and injection

ratio is -5dB.

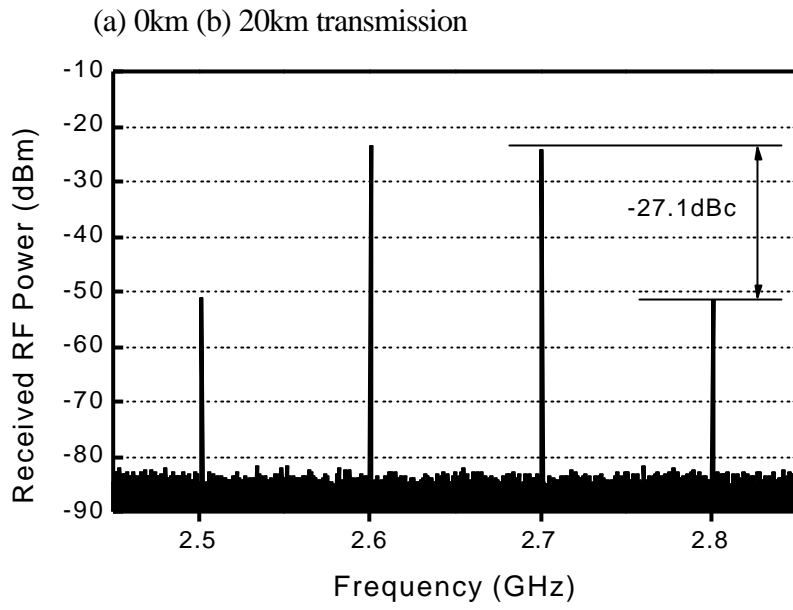


(a)

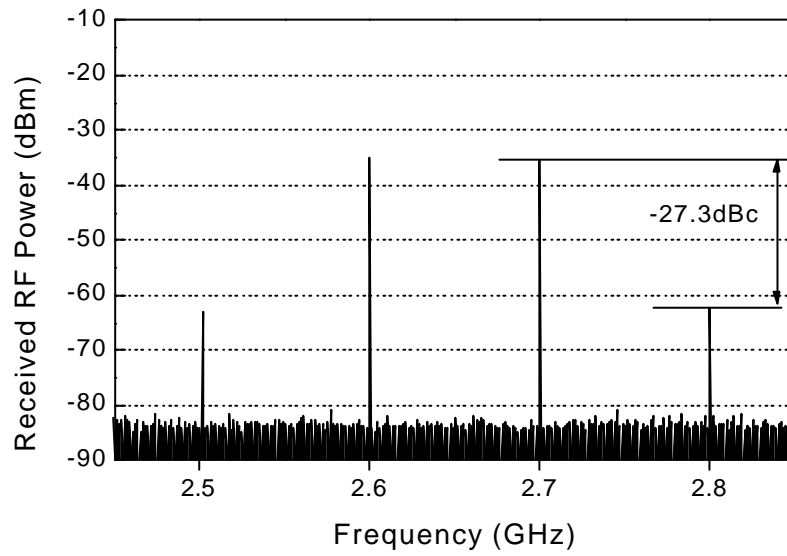


(b)

Figure 4-8. Measured RF power spectra for the free-running FP-LD directly modulated by a two-tone RF signal ($f_1 = 2.6$ GHz, $f_2 = 2.7$ GHz).



(a)



(b)

Figure 4-9. Measured RF power spectra for the injection-locked FP-LD directly modulated by a two-tone RF signal ($f_1 = 2.6$ GHz, $f_2 =$

2.7GHz). (a) 0km (b) 20km transmission

4-9(a), (b)), IMD3 is -27.1 dBc at 0 km and -27.3 dBc at 20 km. On the contrary, in this case, IMD3 decreases by 0.2 dB. Fig. 4-10 shows optical spectra measured by Fabry-Perot interferometer for the free-running and injection-locked FP-LD directly modulated by a two-tone RF signal. Injection-locked FP-LD has almost the same spectrum as shown Fig.4-4 for the injection-locked DFB-LD.

In Fig. 4-11(a), the received RF powers at the fundamental and IMP3 frequencies are plotted for the free-running states. The received RF powers at the fundamental and IMP3 frequencies show a significant fluctuation, while the received RF powers of free-running DFB-LD decrease monotonously. The fluctuation shown by the free-running state is related to the modal dispersion of FP-LD [25]. Fig. 4-11(b) shows that the IMD3 variation for the free-running FP-LD is severe due to the power fluctuation at the fundamental and IMP3 frequencies. On the contrary, in injection-locked FP-LD as shown in Fig 4.12(a), powers at fundamental and IMP3 frequencies decrease almost at the same rate, and the IMD3 is bounded within about 2dB for the entire transmission range (Fig. 4-12(b)), which is quite comparable with that of the injection-locked DFB-LD.

In this section, the dispersion-induced IMD3 variations of directly modulated DFB- / FP-LD over fiber transmission are investigated and the IMD3 can be reduced by optical injection locking of both lasers. IMD3s for free-running semiconductor lasers are degraded due to the combined effect of the semiconductor laser nonlinearities and fiber dispersion. But, in the injection-locked case, semiconductor laser nonlinearities are suppressed, and

the influence of fiber dispersion can be much reduced. In our experiments,

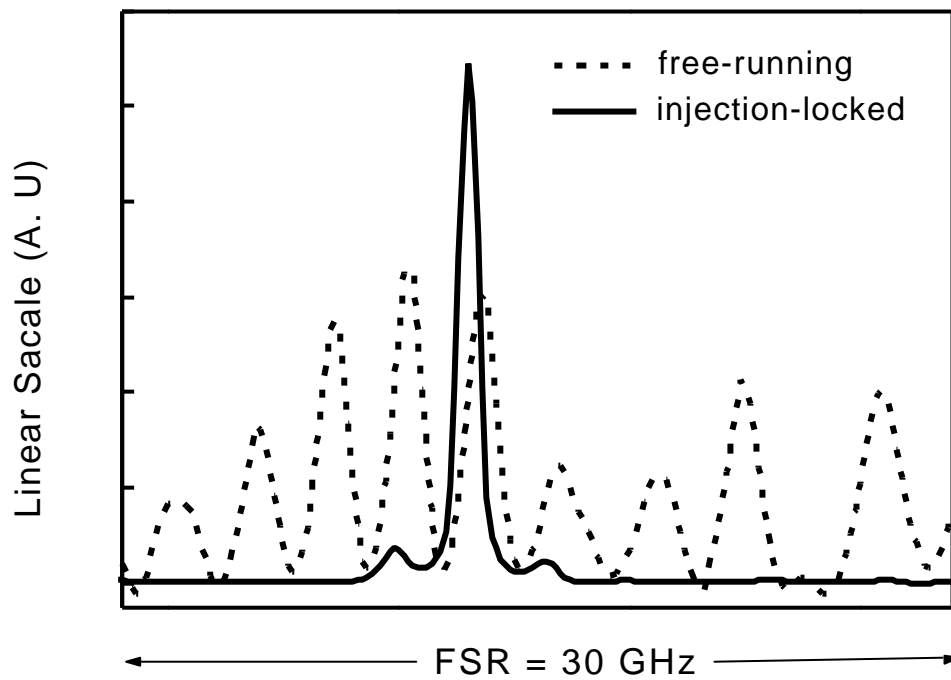


Figure 4-10. Optical spectra measured by Fabry-Perot interferometer for the free-running and injection-locked FP-LD directly modulated by a two-tone RF signal ($f_1 = 2.6$ GHz, $f_2 = 2.7$ GHz)

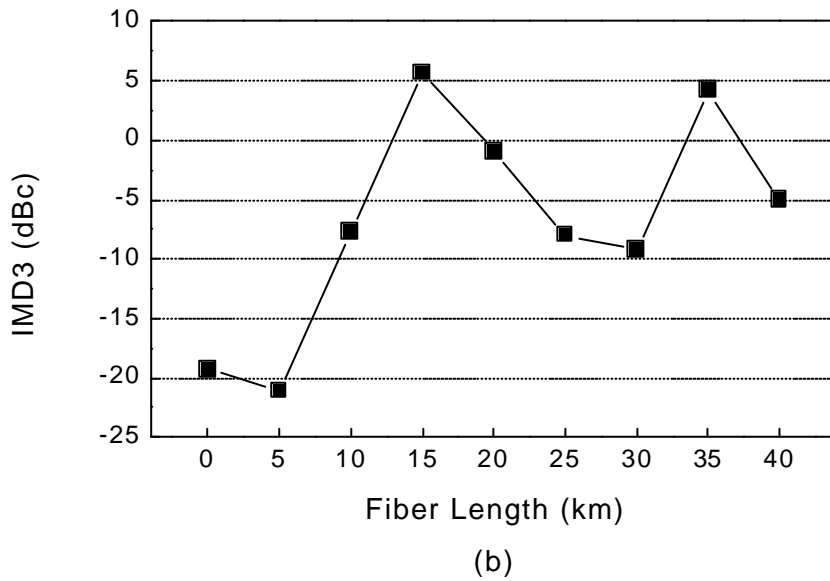
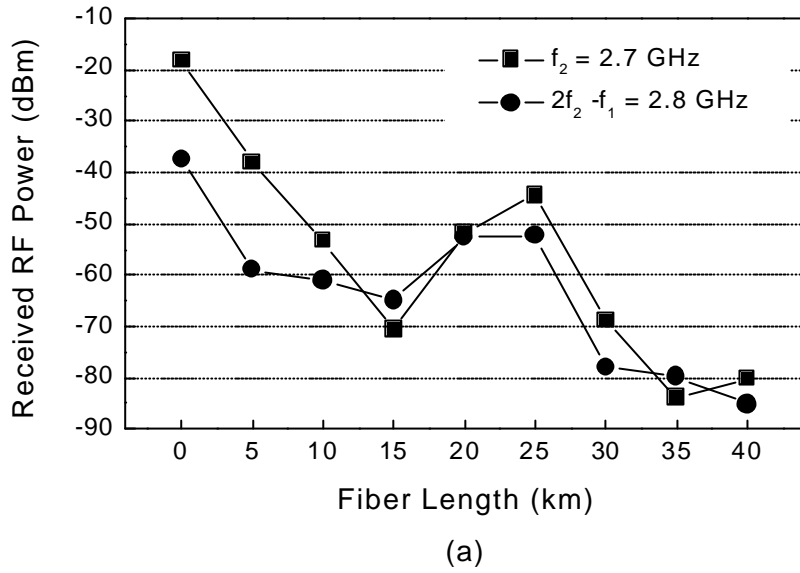
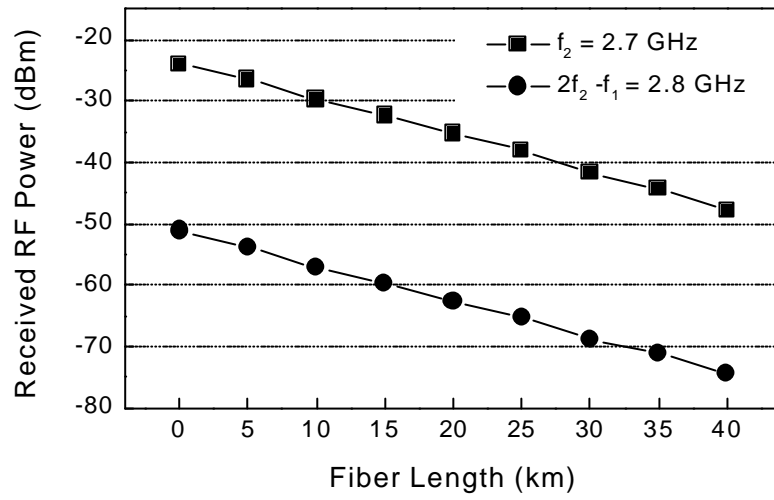
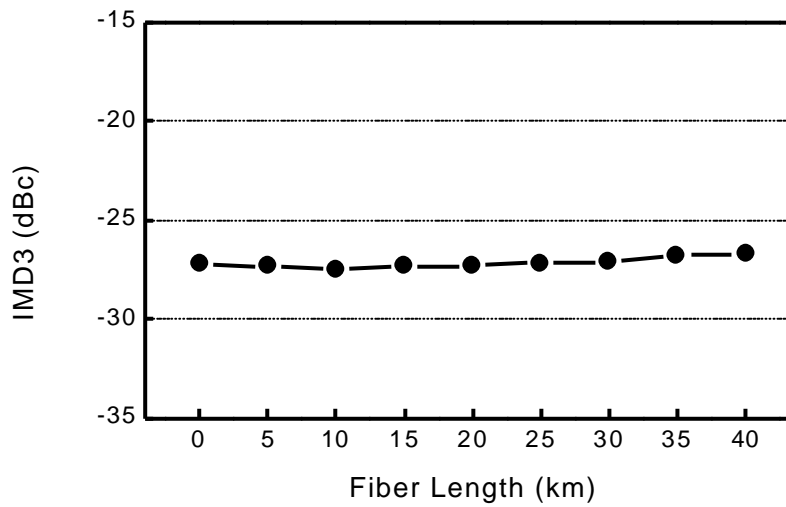


Figure 4-11. (a) Received RF power at f_2 and $2f_2 - f_1$ versus fiber length
 (b) IMD3 versus fiber length for the free-running state.



(a)



(b)

Figure 4-12. (a) Received RF power at f_2 and $2f_2 - f_1$ versus fiber length
 (b) IMD3 versus fiber length for the injection-locked state

16.3 dB reduction in IMD3 for DFB-LD and 21.64 dB reduction for FP-LD can be achieved with injection locking, and IMD3 variation was bounded within ~2 dB for up to 40km transmission as shown in Fig. 4-13(a) and (b).

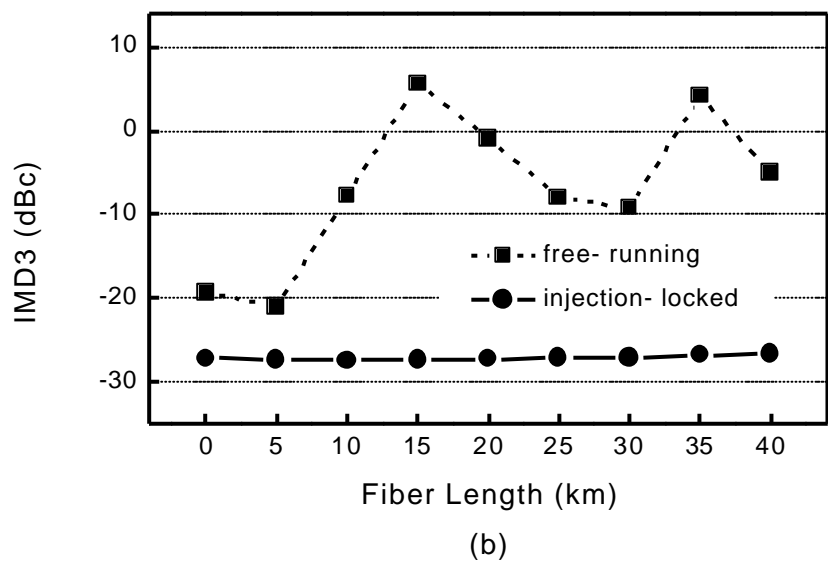
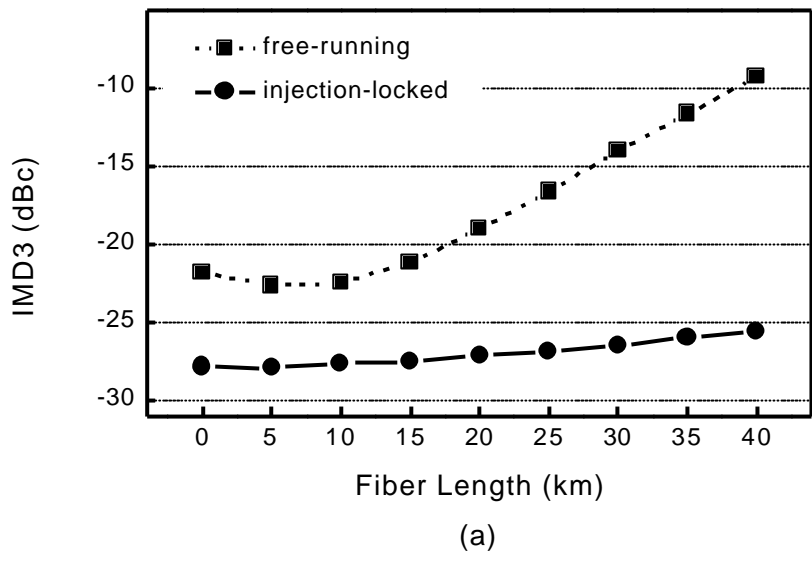


Figure 4-13. Fiber dispersion-induced IMD3 reduction by optical injection locking. (a) DFB-LD (b) FP-LD

V. Conclusion

The injection locking of semiconductor lasers can be used in many optical communication systems because it is a good method to improve semiconductor laser characteristics such as frequency chirping reduction, partition noise reduction, linewidth narrowing and relaxation oscillation frequency increase. The range for the stable locking regime can be determined by the stability analysis of the rate equation. Outside the locking region, no stationary solutions exist and the laser shows beat phenomena. Within the locking region, which is divided into dynamically unstable and stable region, locking phenomena can be occurred. In the unstable region, the SL exhibits the unstable locking characteristics such as pulsation close to the resonance frequency of the free-running laser. On the other hand, in the dynamically stable locking range, the laser is in a stable-locked state and the output power of the injection-locked SL laser is centralized at the frequency of the ML.

From the above locking characteristics, the effects of optical injection locking on the nonlinear distortions of a directly modulated DFB-LD are investigated by numerical simulations. IMD3 of the injection-locked DFB-LD can be much reduced due to the relaxation oscillation frequency increase and the resulting SFDR also be increased from $53 \text{ dB} \cdot \text{MHz}^{2/3}$ to $56.5 \text{ dB} \cdot \text{MHz}^{2/3}$. Furthermore, the injection locking bandwidth of FP-LD is investigated, and the first experimental demonstration on the IMD3 suppression is made at the different injection target modes of FP-LD. The stable-injection locking bandwidth becomes larger as the increase of the ML injection power. At the same ML injection power, the maximum injection locking bandwidth is

achieved in a higher mode. For the injection-locked states into different injection target modes, experimental measurements of IMD3 reduction is performed. It is showed for the first time that the IMD3 reductions are achievable at any target mode injection locking. Consequently, choosing an appropriate injection target mode can enlarge stable locking bandwidth to ~ 32 GHz , reduce the IMD3 by ~ 10 dB.

The fiber dispersion-induced IMD3 variations for the free-running and injection-locked DFB- / FP-LD are investigated, experimentally. When the semiconductor laser is directly modulated by RF signals, modulated optical signal is broadened mainly by laser frequency chirp. Harmonic and intermodulation products are produced by the broadened optical signal, and vary during transmission by fiber dispersion and loss. This leads to IMD3 increase. On the other hand, the injection-locked semiconductor lasers have the improved laser dynamics such as the relaxation oscillation frequency increase and the reduced frequency chirping, and produce the smaller HPs and IMPs. Thus, at no transmission, the significant IMD3 reduction can be achieved, and the optical spectra under the direct modulation become narrower. Since the narrow optical spectra get less affected by the fiber chromatic dispersion, fiber dispersion-induced IMD3 of the injection-locked DFB-LD is not degraded over fiber transmission. Consequently, IMD3s for free-running semiconductor lasers are degraded due to the combined effect of the semiconductor laser nonlinearities and fiber dispersion. But, in the injection-locked case, semiconductor laser nonlinearities are suppressed, and the influence of fiber dispersion can be much reduced.

This thesis is mainly focused on the IMD3 reduction caused by semi-

conductor laser nonlinearities and fiber dispersion. By employing optical injection locking technique, both the IMD3 of the optical light source and the dispersion-induced IMD3 over fiber transmission can be much reduced. In our experiments, 16.3 dB reduction in IMD3 for DFB-LD and 21.64 dB reduction for FP-LD can be achieved with injection locking, and IMD3 variation was bounded within ~ 2 dB for up to 40km. Theoretical and numerical analysis on the dispersion-induced IMD3 of FP-LD remains as future works.

IV. References

- [1] J. Le Bihan and G. Yabre, "FM and IM Intermodulation Distortions in Directly Modulated Single-Mode Semiconductor Lasers," *IEEE J. Quantum Electron.*, vol. 40, no 4, pp. 899-904, 1994.
- [2] G. J. Meslener, "Chromatic Dispersion Induced Distortion of Modulated Monochromatic Light Employing Direct Detection," *IEEE J. Quantum Electron.*, vol. 20, no 10, pp. 1208-1216, 1984.
- [3] K. Y. Lau and A. Yariv, "Intermodulation distortion in a directly modulated semiconductor injection laser," *Appl. Phys. Lett.*, vol. 45, pp. 1034-1036, 1984.
- [4] D. B. Crosby and G. J. Lampard, "Dispersion-Induced Limit on the Range of Octave Confined Optical SCM Transmission System," *IEEE Photon. Technol. Lett.*, vol. 6, no 8, pp. 1043-1045, 1994.
- [5] C. S. Ih and Wanyi Gu, "Fiber Induced Distortions in a Subcarrier Multiplexed Lightwave System," *IEEE J. Sel. Areas in Commun.*, vol. 8, no 7, pp. 1296-1303, 1990.
- [6] D. Pastor, J. Capmany and J. Marti, "Reduction of Dispersion Induced Composite Triple Beat and Second-Order Intermodulation in Subcarrier Multiplexed Systems Using Fiber Gratin Equalizers," *IEEE Photon. Technol. Lett.*, vol. 9, no 9, pp. 1280-1282, 1997.
- [7] S. Kaneko, A. Adachi and J. Yamashita, "A Compensation Method for Dispersion-Induced Third-Order Intermodulation Distortion Using an Etalon," *J. Lightwave Technol.*, vol. 14, no. 12, pp. 2786-2792, 1996.
- [8] G. Y. Yabre and J. L. Bihan, "Reduction of nonlinear distortion in directly modulated semiconductor lasers by coherent light injection," *IEEE J. Quantum Electron.*, vol. 33, no 7, pp. 1132-1140, 1997.

- [9] X. J. Meng, T. Chau, and M. C. Wu, "Improved intrinsic dynamic distortions in directly modulated semiconductor lasers by optical injection locking," *IEEE Trans. Microwave Theory Techniques*, vol.47, no7, pp. 1172-1176, 1999.
- [10] R. Lang, "Injection locking properties of a semiconductor laser with external light injection," *IEEE J. Quantum Electron.*, vol. 18, no 6, pp. 976-983, 1982.
- [11] G. Yabre, "Effect of relatively strong light injection on the chirp-to-power ratio and the 3dB bandwidth of directly modulated semiconductor lasers," *J. Lightwave Technol.*, vol. 14, no. 10, pp. 2367-2373, 1996.
- [12] S. Mohrdiek, H. Burkhard, and H. Walter, "Chirp Reduction of Directly Modulated Semiconductor Lasers at 10 Gb/s by strong CW Light Injection," *J. Lightwave Technol.*, vol. 12, no. 3, pp. 418-424, 1996.
- [13] F. Mogensen, H. Olesen, and G. Jacobsen, "Locking Conditions and Stability Properties for a Semiconductor Lasers with External Light Injection," *IEEE J. Quantum Electron.*, vol. 21, no 7, pp. 784-793, 1985.
- [14] J. Troger, P.-A. Nicati, L. Thevenaz, and Ph. A. Robert, "Novel Measurement Scheme for Injection-Locking Experiments," *IEEE J. Quantum. Electron.*, vol. 35, no. 1, pp. 32-38, 1999.
- [15] B. Wilson, Z. Ghassemlooy, and I. Darwazeh, *Analogue OPTICAL FIBRE communications, The Institution of Electrical Engineers*, pp. 177-227, 1995.
- [16] W. I. Way, "Large Signal Nonlinear Distortion Prediction for a Single-mode Laser Diode under Microwave Modulation," *J. Lightwave Technol.*, vol. 5, pp. 305-315, 1987.
- [17] J. Helms, "Intermodulation and Harmonic Distortions of Laser Diodes with Optical Feedback," *J. Lightwave Technol.*, vol. 9, pp. 1567-1575, 1991.
- [18] H. M. Salgado and I. J. O'Reilly, "Experimental Validation of Volterra Series

- Nonlinear Modeling for Microwave Subcarrier Optical Systems,” *Proc. Inst. Elect. Eng.*, vol. 134, no 4, pp. 209-213, 1996.
- [19] J. C. Cartledge, “Theoretical Performance of Multigigabit-Per-Second Lightwave Systems Using Injection-locked Semiconductor Lasers,” *J. Lightwave Technol.*, vol. 8, no. 7, pp. 1017-1022, 1996.
- [20] I. Petibon, P. Gallion, G. Debarge, and C. Chabran, “Locking Bandwidth and Relaxation Oscillations of Injection-locked Semiconductor Laser,” *IEEE J. Quantum Electron.*, vol. 24, pp. 148-154, 1988.
- [21] J. Wang, M. K. Halder, L. Li, and F. V. C. Mendis, “Enhancement of Modulation bandwidth of Laser Diodes by Injection Locking,” *IEEE Photon. Technol. Lett.*, vol. 8, pp. 34-36, 1996.
- [22] J. M. Luo and M. Osinski, “Multimode small-signal analysis of side-mode injection-locked semiconductor lasers,” *Jpn. J. Appl. Phys.*, vol.31, pp. L685-L688, 1992.
- [23] Y. Hong and K. A. Shore, “Locking characteristics of a side-mode injected semiconductor laser,” *IEEE J. Quantum Electron.*, vol. 35, pp. 1713-1717, 1999.
- [24] J. C. Cartledge and A. F. Elrefaie, “Effect of Chirping-Induced Waveform Distortion on the Performance of Direct Detection Receivers Using Traveling-Wave Semiconductor Optical Preamplifiers,” *J. Lightwave Technol.*, vol. 9, pp. 209-219, 1991.
- [25] S. Hunziker and W. Baechtold, “Fiber dispersion induced nonlinearity in fiber-optic links with multimode laser diodes,” *J. Lightwave Technol.*, vol. 9, pp. 371-373, 1997.

Injection-locked

Subcarrier multiplexed (SCM)

harmonic intermodulation distortion
SCM .
locking
injection locking .
rate equation injection-
locked locking
Fabry-Perot laser diode (FP-LD) injection locking bandwidth
third-order intermodulation distortion (IMD3) FP-LD
. FP-LD injection locking bandwidth IMD3 injection-
locked FP-LD
injection locking bandwidth IMD3
. , 가 IMD3
free-running injection-locked
. free-running IMD3
가 .
, injection-locked relaxation oscillation frequency 가
frequency chirping dynamics 가 free-running

IMD3 가

IMD3 가 .

: , intermodulation ,
optical injection locking